coatings

MDPI

Review

Nanomaterials and Equipment for Chemical–Mechanical Polishing of Single-Crystal Sapphire Wafers

Shaoping Li [1,†], Jieni Fu [2,†], Zhaobo He [1,*], Yue Luo [1] and Shuilin Wu [2,*]

[1] Hubei Sinophorus Electronic Materials Co., Ltd., Xiaoting Avenue 66-3#, Xiaoting District, Yichang 443007, China; lisp@sinophorus.com (S.L.); luoyue@sinophorus.com (Y.L.)
[2] The Key Laboratory of Advanced Ceramics and Machining Technology by the Ministry of Education of China, School of Materials Science & Engineering, Tianjin University, Tianjin 300072, China; jienifu@tju.edu.cn
* Correspondence: zhaobo_he@sinophorus.com (Z.H.); shuilinwu@tju.edu.cn (S.W.)
† These authors contribute equally to this work.

Abstract: Single-crystal sapphire (α-Al_2O_3) has been widely used in semiconductor, optics, communication, national defense, and other fields. Before application, an ultra-smooth surface which is scratch free and subsurface damage free is essential. Furthermore, the sapphire has unique qualities such as significant rigidity and chemical stability, which make it extremely arduous to process. Chemical mechanical polishing (CMP) is recognized as the final process to reduce the roughness and eliminate surface defects of a sapphire surface. In this review, the materials and equipment used for the chemical polishing of a sapphire wafer are summarized, and the surface nanoscale changes of sapphire wafer are reviewed from the angles of regulating polishing-process parameters, composition of polishing slurry including that which is nano-abrasive, a pH regulator, a complexing agent, and other additives, as well as hybrid CMP technologies. The outlook and future applications are also summarized.

Keywords: single-crystal sapphire; chemical mechanical polishing; nanomaterials; surface roughness

check for updates

Citation: Li, S.; Fu, J.; He, Z.; Luo, Y.; Wu, S. Nanomaterials and Equipment for Chemical–Mechanical Polishing of Single-Crystal Sapphire Wafers. *Coatings* **2023**, *13*, 2081. https://doi.org/10.3390/coatings13122081

Academic Editor: Roberto Montanari

Received: 7 November 2023
Revised: 6 December 2023
Accepted: 7 December 2023
Published: 14 December 2023

Copyright: © 2023 by the authors. Licensee MDPI, Basel, Switzerland. This article is an open access article distributed under the terms and conditions of the Creative Commons Attribution (CC BY) license (https://creativecommons.org/licenses/by/4.0/).

1. Introduction

Semiconductor materials have provided a strong boost to the development of modern science and technology, and their development have also promoted the development of the world's industries, industries that greatly enhance the productivity of society [1–3]. Semiconductor materials can be divided into silicon-based semiconductors and compound semiconductors [4–6]. The global semiconductor chip market, dominated by silicon wafers, is expected to exceed $772.03 billion by 2030 [7]. The main compound semiconductors are gallium arsenide (GaAs), indium phosphide (InP), silicon carbide (SiC), gallium nitride (GaN), and so on [8–11]. Among them, GaN, a promising material, has been widely used in various photoelectric devices [11]. However, the growth rate of GaN single crystal is slow, the crystal growth is difficult, and the cost is high [12]. Therefore, GaN single crystals cannot be directly prepared, and heteroepitaxy can only be grown on other substrates. The most common substrate for growing gallium nitride single crystals is sapphire wafer [12]. As an anisotropic material, single-crystal sapphire (α-Al_2O_3) can be divided into C-, A-, R-, and M-plane sapphire [13–15]. Diverse crystallographic planes possess distinctive performance, and their application areas are also different. For instance, C- and M-plane sapphires have been put to extensive use as light-emitting diode (LED) substrates, and particularly C-planar sapphire substrates can grow GaN epitaxially, so they are extensively applied as substrate materials for GaN-based LEDs [16–18]. A-plane sapphire is normally applied as an optical window material, such as a window material for high-intensity lasers and infrared devices [19,20]. R-plane sapphire is preferred for the heteroepitaxial deposition of silicon, which is used to fabricate semiconductor, microwave, and microelectronic integrated circuits [21]. To sum up, sapphire has splendid chemical, mechanical, and

optical unique properties, such as high temperature resistance, fast thermal conductivity, high hardness, high light transmission, good chemical stability, etc. [22–24]. Therefore, as shown in Figure 1, sapphire is heavily applied in communications, electronics, aerospace, optics, biological engineering, and other high-end technical fields [25–27]. The preparation process of sapphire wafers is similar to that of silicon carbide wafers, in that large-size and high-quality single-crystal sapphire crystals are grown in a long crystal furnace [28], and then processed into the final substrate through processes such as orientation, rod removal, tumbling, wire sawing [29], double-sided polycrystalline diamond grinding, chamfering, chemical–mechanical polishing (CMP), cleaning, and post-processing [30]. Among them, the final surface quality of the wafer is determined by CMP. At present, sapphire wafer also has many possible surface processing methods, such as femtosecond laser micromachining, focused ion beam processing, laser interference lithography, and so on [31–33]. However, the premise that sapphire wafer can be surface treated is so that the surface quality of the sapphire substrate meets requirements. With the speedy evolution of the semiconductor technique, the processing productivity and surface quality of sapphire substrates are subject to higher requirements, including having high processing efficiency, an ultra-smooth wafer surface, no defects, no damage, and a value of surface roughness (Ra) below the danami level [34]. For example, sapphire substrates require a surface roughness (Ra) between 0.2 and 1 nm at a high material removal rate [34], whereas, in view of the significant rigidity, brittleness, and chemical inertness of sapphire, there are two major problems of sapphire CMP. First, the polishing efficiency of sapphire is too low, and the polishing time is too long, which accounts for 70% of the total processing time [35]. Second, high surface roughness and deep scratches caused by the grinding process are difficult to reduce and remove quickly in the CMP step [36,37]. Therefore, it is a huge challenge to reach a satisfactory CMP result. However, in the face of the increasing demand for sapphire wafer, the question of how to solve the current problems in the sapphire CMP process is very important [35].

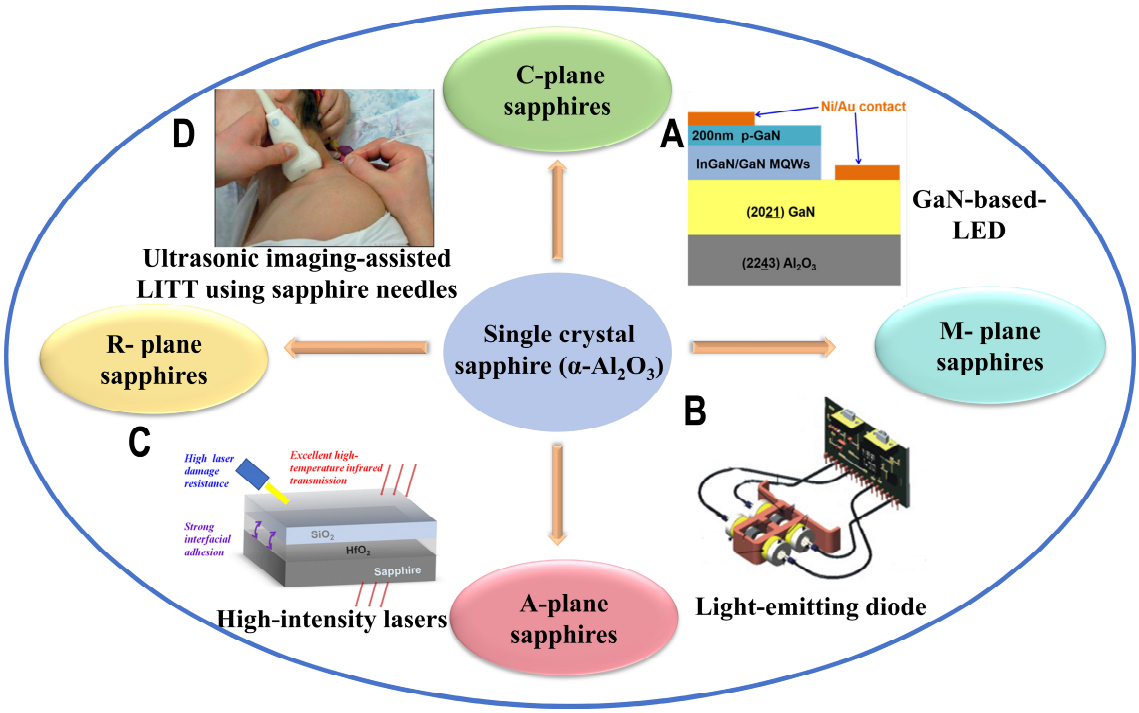


Figure 1. Classification and applications of single-crystal sapphire. (**A**) GaN-based LED. Adapted with permission [16]. Copyright 2017, American Chemical Society. (**B**) Light-emitting diode. Adapted with permission [25]. Copyright 2018, Elsevier B.V. (**C**) High-intensity lasers. Adapted with permission [19]. Copyright 2021, American Chemical Society. (**D**) Ultrasonic-imaging-assisted LITT using sapphire needles. Adapted with permission [26]. Copyright 2018, Elsevier B.V.

Walsh et al. put forward the concept of CMP in 1965 [38]. CMP has become a globally recognized flattening technique, which can generate explanate surfaces without blemishes [39–44]. In the process of CMP, the material to be polished is fixed on the polishing head, and it is fully in contact with the polishing cushion by applying appropriate stress to the polishing head (Figure 2) [45]. Then, the polishing head and polishing disc are rotated at a certain speed and direction under the drive of the motor, and the polishing slurry is added to the polishing cushion with an appropriate flow rate through a feeding system of the polishing machine, which is evenly distributed to the entire polishing cushion using centrifugal force. The chemical reagents in the polishing slurry will soften the polished material to produce a softer film layer, which is then removed using mechanical friction, so that effective polishing is achieved through the repeated film-forming mechanical removal process. At the end of polishing, the polished material is cleaned, and finally the material with an ultra-precise surface is prepared. According to the polishing process, the CMP polishing system is composed of polishing equipment and polishing consumables, among which the polishing consumables are composed of a polishing pad, polishing slurry, and post-cleaning fluid. Polishing slurry is constituted of abrasives, oxidizers, pH adjusters, surfactants, and dispersants [46]. Among them, abrasives are the nanomaterials used in sapphire CMP, which can be divided into nano-silicon oxide (SiO_2), nano-cerium oxide (CeO_2), nano-alumina (Al_2O_3), and so on [47]. Therefore, there are many factors affecting the polishing efficiency of sapphire: from the perspective of polishing equipment, there are factors such as polishing pressure and polishing speed; from the perspective of polishing materials, there are various affects such as the type of abrasive and various additives in polishing slurry and so on. Therefore, many researchers are constantly looking for methods to boost the polishing efficiency and superficial mass of sapphire from the above factors.

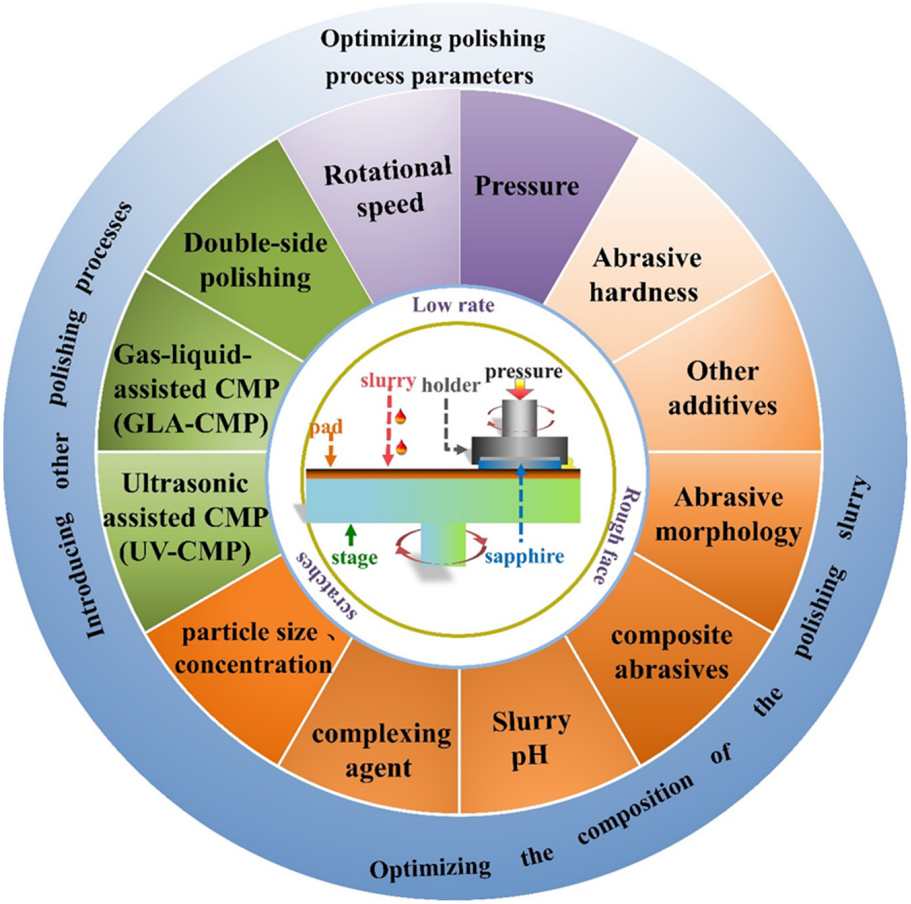


Figure 2. The strategies to improve sapphire CMP.

In this review, we highlight the latest advances in CMP technology in sapphire wafers and summarize and analyze the mechanism of sapphire CMP polishing. Based on the composition of the sapphire CMP polishing system, a strategy to improve the efficiency of sapphire CMP polishing was proposed (Figure 2). Specifically, the first method is to improve the polishing pressure and speed by adjusting the parameters of the polishing equipment to improve the pressure on the wafer and the rotation speed of the polishing disc; in general, with the increase of pressure and rotational speed, the polishing rate of the sapphire will increase. The second method is to appropriately increase the hardness of the abrasive; with the increase of abrasive hardness, it is easier to grind off the hydrated layer of the sapphire surface, thereby improving the polishing rate. The third method is to change the size and concentration of the abrasive under the same conditions; with the increase of size and concentration of the abrasive, the effective abrasive contact with sapphire will increase, so the polishing rate will also increase. The fourth method is to change the shape of the abrasive; in general, an irregular abrasive shape will be more in contact with the sapphire than the spherical abrasive under the same conditions, so it will also improve the polishing rate. The fifth method is the construction of mixed abrasives, mixed abrasives will combine the advantages of different abrasives to achieve a good polishing effect. The sixth method is to change the pH value of the polishing slurry by adjusting the amount of pH regulator. The pH value affects the polishing rate of the sapphire by changing the zeta potential of the abrasive and the formation of the hydration layer on the sapphire surface. Generally speaking, the polishing rate of the sapphire will be higher under alkaline conditions. The seventh method is to change the type of chelating agent; chelating agent combines with the hydration layer formed on the surface of the sapphire to form a chelate which is soluble and easily worn by abrasive to improve the polishing efficiency of sapphire. The eighth method is to add other additives, such as metal salts, surfactants, or other catalysts; the addition of additives will change the chemical action between the abrasive and sapphire, thereby improving the polishing efficiency. The ninth method is the introduction of new polishing auxiliary processes, such as ultrasonic assistance, gas assistance, and a double-sided polishing process, the introduction of new auxiliary processes can further improve the polishing efficiency. Ulteriorly, we look forward to the future development direction of sapphire CMP polishing technology. It is hoped that it can provide research ideas for researchers to further develop more efficient sapphire CMP.

2. The Mechanism of Sapphire Polishing

From the above introduction, sapphire has A-, C-, M- and R-plane four-crystal planes (Figure 3) [48]. According to the research of Cao et al., C-plane sapphire had the lowest bond energy due to the smallest spacing between adjacent crystal faces [48]. The lower the binding energy, the easier the material could be removed. The experimental consequences also displayed that under the same conditions, the MRR of the C-surface sapphire was 5.93 nm/min, the Ra was 0.307 nm, and the polishing effect was the best.

The above research is only an experimental and simple theory to prove that the polishing rate of different crystal planes of sapphire is not the same, however, its polishing mechanism has not been further studied. Zhu et al. considered that one of the reasons for the polishing anisotropy of the C-, A-, and M-plane of sapphire was that no hydration layer was formed during the polishing process of A- and M-plane sapphire [36]. However, the diaspore [AlO(OH)] hydration layer was formed on the surface of the C-plane sapphire. Haas's experiments had proved that at high temperature and pressure, the epitaxial growth of diaspore occurred on the surface of the corundum substrate, but not on other planes [36]. The reason could be attributed to the topotactical relationship between α-Al_2O_3 and diaspore, both of which were hexagonal and close packed [36]. In other words, the coordination number of aluminum ions was six for both α-Al_2O_3 and diaspore, while in all other forms of alumina and aluminum hydrates the coordination numbers of aluminum ions were mixtures of six and four. Whereas gibbsite and boehmite were cubic [36]. When

the abrasive and hydration layers came into close contact under polishing pressure and shearing, they adhered to each other. Further shearing might allow the particles to "tear" the bound hydrated layer and even promoted further removal of the particle front. In a study by Shi and Zhou et al., aluminum (Al) atoms and oxygen (O) atoms formed the Al-O layer in sapphire crystal, so the sapphire was assembled through a periodic stacking sequence of Al-O layers (Figure 4A) [49–52]. The AFM data showed that the C-plane sapphire presented an atomic step–step morphology, and the average height of the terrace was 0.22 nm, which was the same as the theoretical thickness of the Al-O layer (0.216 nm) (Figure 4B,C) [51]. During sapphire CMP, the hydration layer was formed on the surface of the terraces as shown in Formulas (1) and (2), which was then removed using an abrasive with the help of mechanical force.

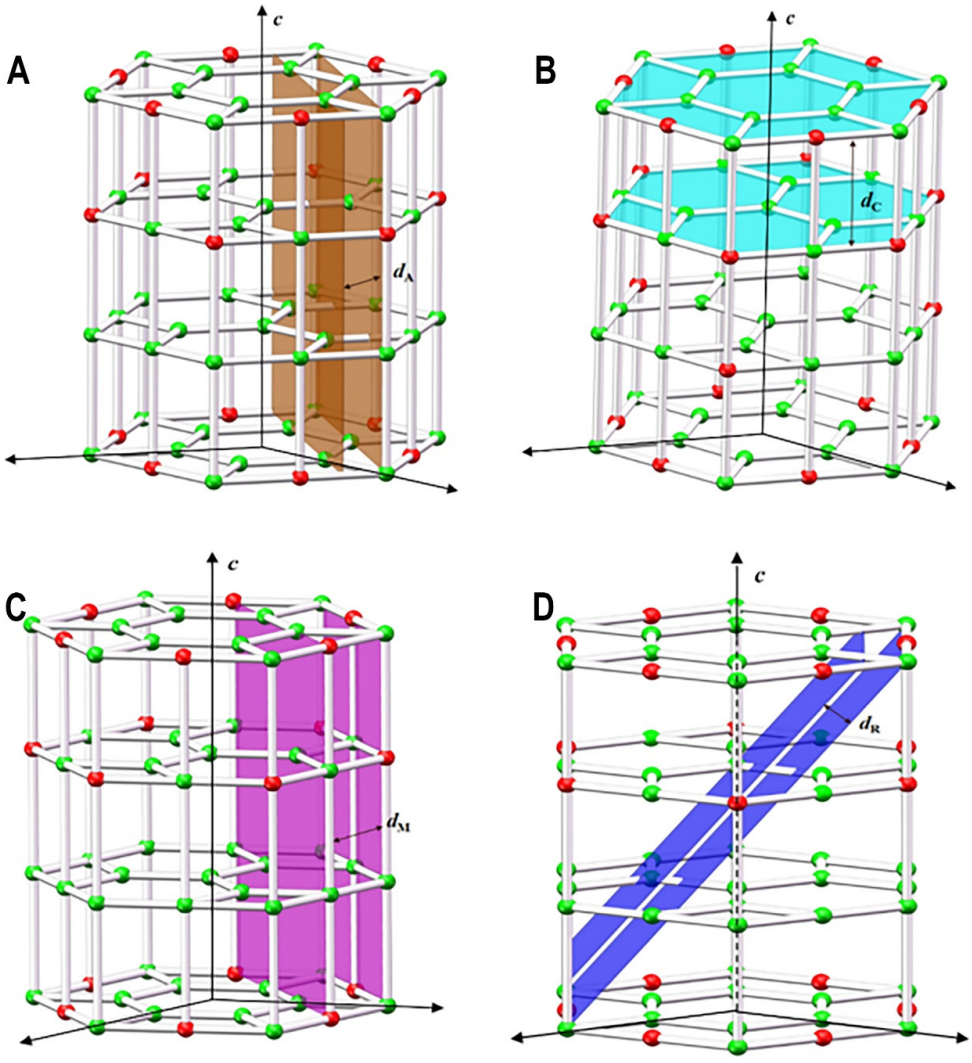


Figure 3. Crystal patterns of (**A**) A-plane, (**B**) C-plane, (**C**) M-plane, and (**D**) R-plan of sapphire. Adapted with permission [48]. Copyright 2020, MDPI.

Therefore, the abrasive plays a decisive role in the effect of the sapphire CMP. Sapphire polishing slurry can be divided into Al_2O_3-based and SiO_2 sol-based polishing slurry based on its different abrasives, and the polishing mechanism of these two kinds of polishing slurry is different. According to the above research, when the abrasive is Al_2O_3, Al_2O_3 can hydrate in a similar way to sapphire because they have the same crystal structure [48]. Adhesion occurs when two surfaces are in close contact under polishing pressure and shearing. In the meantime, the irregular parts and hydration layers on the sapphire surface

was mechanically split and wiped off on account of the irregular shape and large size of Al_2O_3.

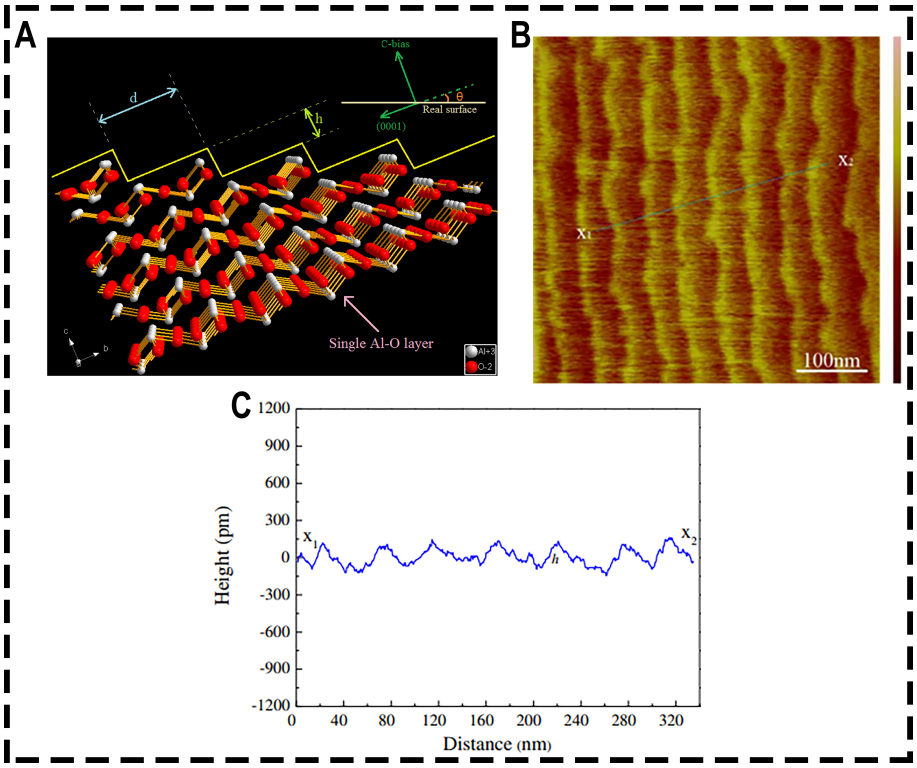


Figure 4. An atomic model described the principle of step-terrace structure (**A**) was also provided. The scale bar was 1 nm. The real value of θ was below 0.5°. AFM image of atomic step. Terrace structure on sapphire substrate (**B**), and the section curve of terraces (**C**) [51]. Adapted with permission. Copyright 2015, Elsevier B.V.

$$Al_2O_3 + H_2O = 2AlO(OH) \quad (1)$$

$$Al_2O_3 + 3H_2O = Al(OH)_3 \quad (2)$$

$$2SiO_2 + H_2O + 2AlO(OH) = Al_2Si_2O_7{\cdot}2H_2O \quad (3)$$

$$2SiO_2 + Al(OH)_3 + AlO(OH) = Al_2Si_2O_7{\cdot}2H_2O \quad (4)$$

$$2SiO_2 + 2H_2O + Al_2O_3 = Al_2Si_2O_7{\cdot}2H_2O \quad (5)$$

$$(SiO_2)_x + 2H_2O = (SiO_2)_{x-1} + Si(OH)_4 \quad (6)$$

$$Si(OH)_4 + 2Al^{3+}{}_{sur} + H_2O = Al_2SiO_5 + 6H^+ \quad (7)$$

$$Si(OH)_4 + 2AlO^-{}_{sur} = Al_2SiO_5 + 2OH^- + H_2O \quad (8)$$

When the abrasive is silica sol, most researchers believe that silica reacts with the sapphire or the hydrated layer on the surface of the sapphire to form a soft layer (mainly $Al_2Si_2O_7{\cdot}2H_2O$), as shown in the Formulas (3)–(5) above [52,53]. Then, the silica particles

remove the material from the wafer surface through the chemical-bond tension created by their mechanical movement. However, Vovk et al. believed that silica abrasives undergo a chemical reaction, as shown in Formulas (6)–(8), in which a layer of Al_2SiO_5 aluminum silicate at a thickness of 20.5 nm was formed on the surface of sapphire during the CMP process, which was then removed using silica abrasives [54]. Yu et al. also demonstrated the formation of Al_2SiO_5 [55]. All in all, regardless of the compound formed by silica sol and alumina, the recognized mechanism is that at the interface between the abrasive and the sapphire, the solid–solid reaction between the sapphire and the abrasive will occur, forming a soft layer, which is conducive to the removal of the sapphire. Under these circumstances, SiO_2 performs two functions: The first is that SiO_2 reacts with sapphire to produce new adhesion on the sapphire surface. The second is to separate and wipe off the new adhesion on the sapphire surface [53]. In summary, the removal mechanism of sapphire is shown in Figure 5.

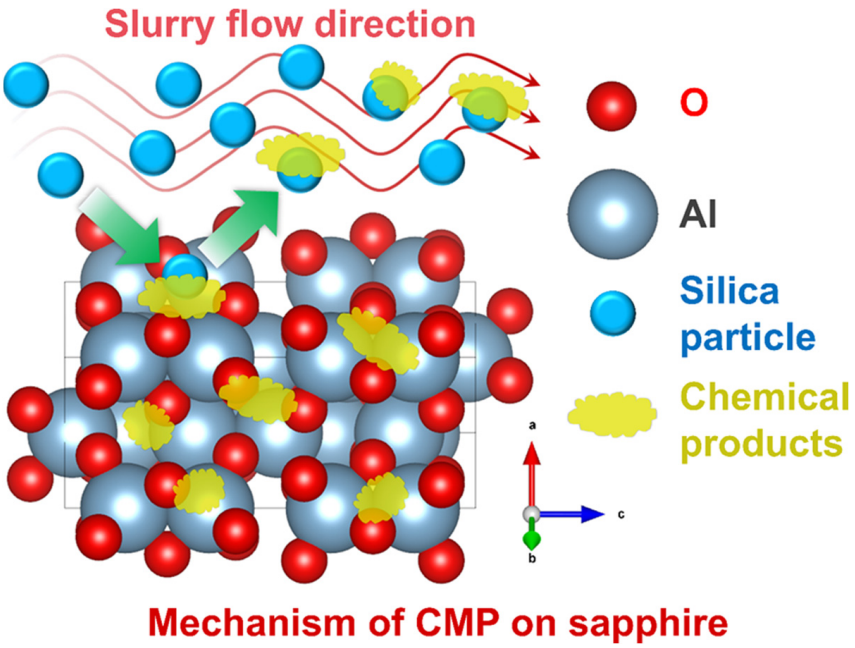


Figure 5. The mechanism of sapphire CMP.

3. The Methods to Boost the Sapphire CMP Efficiency Productivity

According to the composition of the sapphire CMP polishing system, the processing efficiency and surface quality of sapphire CMP can be improved from both the mechanical and chemical aspects. From the mechanical aspect, it is necessary to improve the polishing process, such as by increasing the polishing pressure and polishing speed, and from the chemical aspect it is necessary to optimize the composition of the polishing slurry. For example, by changing the hardness, size, and morphology of abrasives, constructing composite abrasives, changing the pH value of polishing slurry, changing the complexing agent of polishing slurry, and adding other additives. In addition, another method that could be used is the introduction of new polishing auxiliary processes, such as ultrasonic-assisted polishing or gas–liquid-assisted polishing.

3.1. Optimizing Polishing-Process Parameters

It is well known that Preston's empirical formula has been applied to explain the MRR property of CMP [56].

$$\mathrm{MRR} = kPV \tag{9}$$

where k is Preston's constant resting with the chemical and mechanical sides of the process, P is polishing stress, and V is polishing speed [56–59].

Therefore, the removal rate of sapphire is positively correlated with the downforce and speed of the equipment. Many researchers have also proved that polishing pressure and rotational speed have important effects on the performance of CMP [53,56,60–66]. Table 1 lists the influence of polishing pressure and rotational speed on the polishing efficiency of sapphire in some of the literature [53,56,60–65]. The quality of the finished surface will be affected by altering the polishing parameters. For instance, Zhang et al. used silica-based slurry to explore the effects of polishing pressure and rotational speed on the MRR and Ra of the sapphire substrate, and the results were shown in Figure 6A [53]. In the range of pressure and speed researched, MRR increased with the increase of pressure and speed, while Ra decreased first and then increased. When the pressure was 5 psi and the speed was 100 rpm, the lowest surface roughness and medium MRR were obtained. Xu et al. studied the effects of parameters including the downforce and rotational speed on sapphire polishing (Figure 6B) [60]. The experimental results showed that when the downforce was 7 psi, chemical corrosion and mechanical wear were dynamically balanced, and a high MRR and the lowest roughness could be obtained. Zhang et al. also explored the effects of pressure and rotational speed on sapphire CMP, and the results showed that with the increase of rotational speed Ra dropped to the lowest value of 0.56 nm and then rose again (Figure 6C) [62]. At the same time, MRR displayed a linear downward trend at first, and finally increased to the highest value, which was 1.795 μm/h. With the increase of pressure, MRR increased linearly, with a peak value of 2.059 μm/h. Ra first decreased to the lowest 0.548 nm and then increased. From the above research, it can be seen that the processing efficiency and surface quality of sapphire can be effectively improved by increasing the pressure and speed appropriately.

Table 1. The influence of polishing pressure and rotational speed on the polishing efficiency of sapphire.

Pressure (psi)	Rotational Speed (rpm)	MRR (μm/h)	Ra (nm)	Ref.
1, 3, 5, 7	100	MRR increases with increasing pressure	With the change of pressure, it decreases first, reaches the minimum at 5 psi, and then increases	[53]
5	75, 100, 125, 150	MRR increases with increasing rotational speed	With the change of rotational speed, it decreases first, reaches the minimum at 100 rpm, and then increases	[53]
5	75, 100, 125, 150	MRR increases with increasing rotational speed	/	[56]
5, 7, 9, 11	60	MRR increases with increasing pressure	With the change of pressure, it decreases first, reaches the minimum at 7 psi, and then increases	[60]
3.2, 4.17, 5.13, 6.09	10, 20, 30, 40	MRR increases with increasing pressure and rotational speed	With the change of pressure and rotational speed, it decreases first, reaches the minimum, and then increases	[61]
4.06, 5.15, 5.8, 6.5	/	MRR increases with increasing pressure	With the change of pressure, it decreases first, reaches the minimum, and then increases	[62]
/	60, 70, 80, 90	With the change of rotational speed, it decreases first, reaches the minimum, and then increases	With the change of rotational speed, it decreases first, reaches the minimum, and then increases	[62]
2.47, 3.39, 5.04, 6.54, 8.27, 10.01	40	MRR increases with increasing pressure	/	[63]
6.54	20, 30, 40, 50, 60	MRR increases with increasing rotational speed	/	[63]

Table 1. *Cont.*

Pressure (psi)	Rotational Speed (rpm)	MRR (μm/h)	Ra (nm)	Ref.
3, 5, 7, 10	/	With the change of pressure, it increase first, reaches the minimum, and then increases	With the change of pressure, it decreases first, reaches the minimum, and then increases	[64]
1.4, 2.1, 2.8, 3.49, 4.2	/	MRR increases with increasing pressure	With the change of pressure, it decreases first, reaches the minimum, and then increases	[65]

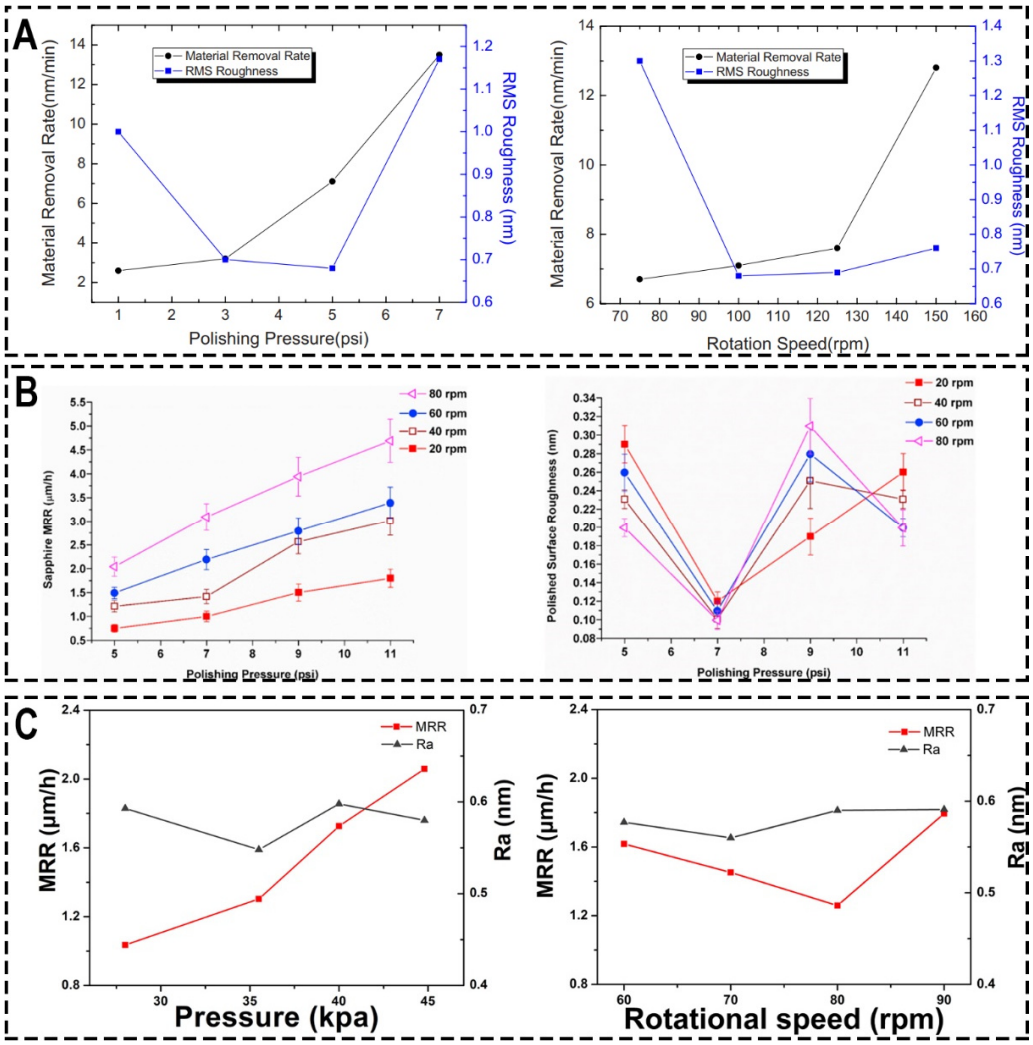


Figure 6. (**A**) MRRs and Ra caused by various polishing pressures and rotating speeds [53]. Adapted with permission. Copyright 2010, The Electrochemical Society. (**B**) MRRs and Ra caused by various polishing pressures and rotating speeds [60]. Adapted with permission. Copyright 2019, Elsevier B.V. (**C**) Effect of pressure and rotating speeds on Ra and MRR after orthogonal CMP experiments on sapphire [62]. Adapted with permission. Copyright 2021, Elsevier B.V.

3.2. Optimizing the Composition of the Polishing Slurry

The change of abrasives and other additives in the polishing slurry is an important factor affecting the chemical reaction of sapphire CMP. Therefore, many scholars have conducted in-depth research on the composition changes of polishing slurry to improve the MRR and surface quality of sapphire CMP.

3.2.1. Changing the Hardness of the Abrasive

The abrasives used for sapphire polishing are mainly diamond, Al_2O_3, SiO_2, boron carbide (B_4C), etc. [36,67–73]. Prior to the use of abrasives, it is valuable to understand the formation mechanism of abrasive nanoparticles. For example, the synthesis mechanism of Al_2O_3 and SiO_2 nanoparticles is such that with the increase of temperature, the oxidation phase nanoparticles in their metal salts will nucleate and grow, thereby producing the final nanoparticles [74]. In the study of Zhu et al., they found that hard abrasives (such as single-crystal and polycrystalline diamond, α-Al_2O_3 and γ-Al_2O_3) could improve the MRR of sapphire, but the Ra of sapphire after polishing was high [36]. In contrast, the Ra of sapphires after polishing with soft abrasives (such as SiO_2) was lower, but the MRR of sapphires also was lower. Furthermore, they studied the effect of different-hardness abrasives on sapphire CMP more comprehensively, and the results as shown in Table 2, which revealed that in the case of the same abrasive size, harder abrasives do not necessarily lead to faster material removal and better surface finish [67]. Abrasives with hardness equal to or less than sapphire, such as α-Al_2O_3 and γ-Al_2O_3, obtained the best surface finish and the highest material-removal efficiency. In the findings of Xiong et al., they found that under the same conditions the Ra of SiO_2-abrasive-polished sapphire was lower than that of silicon carbide (SiC) and Al_2O_3 [70]. It can be seen from the above research, due to the high hardness of Al_2O_3, B_4C, and diamond abrasives, its grinding force on sapphire is strong, and the MRR of sapphire is high. But, they can easily leave deep scratches on the surface of the sapphire, which seriously affects the surface quality of the polished sapphire piece. The hardness of SiO_2 is small; when the SiO_2 is used as an abrasive, the MRR and Ra of sapphire is low. All in all, considering that SiO_2 has the characteristics of easy synthesis, good dispersion, easily modifiable, and, at the same time, when SiO_2 is used as an abrasive the surface state of sapphire is excellent after polishing, and it is not easy to produce scratches and other defects, so SiO_2 is most often applied to the CMP of sapphire as an abrasive [75].

Table 2. The MRR, surface finish, and scratch depth of various abrasives on sapphire CMP in ref. [67].

Abrasive	Size (μm)	Mohs Hardness	MRR of Sapphire (mg/h)	Ra (nm)	Scratch (nm)
Monodiamond	0–0.25	10	0.22 ± 0.04	2.3	12
Polydiamond	0–0.25	10	0.13 ± 0.02	0.5	2
α-Al_2O_3	0.16	9	0.47 ± 0.08	0.4	0.8
α-Al_2O_3	0.2	9	0.43 ± 0.08	0.3	0.8
γ-Al_2O_3	3	8	0.2 ± 0.04	1.0	1
Silica	0.2	7	0.11 ± 0.03	0.4	1.0
ZrO_2	0.4	6.5	0.13 ± 0.01	0.4	1.0
CeO_2	0.64	6	0.00 ± 0.01	16	30

3.2.2. Changing the Particle Size and Concentration of the Abrasive

It is not only the type of abrasive that will affect the polishing effect of the polishing material, but the sapphire CMP efficiency will also be affected by altering particle size and concentration [68,76–84]. Table 3 lists the influence of particle size and the concentration of the abrasive on the polishing efficiency of sapphire in some of the literature [68,77–84]. For instance, Wang et al. used SiO_2 abrasive with particle sizes of 20, 50, 80, and 100 nm for CMP on sapphire, and found that the MRR of sapphire appeared as a linear relationship with silica diameter and increased steeply from 2.02 μm/h to 3.64 μm/h with particle size increasing from 20 nm to 100 nm (Figure 7A) [68]. When the particle size is 100 nm, the MRR increased from 0 to 4.97 μm/h with the increase of concentration from 0 to 40 wt%. Zhang et al. investigated the influence of the particle size and concentration of silica sol on sapphire CMP [77]. In general, MRR is strongly dependent on abrasive concentration, but also changes with particle size. Figure 7B disclosed that the larger the concentration, the greater the sapphire MRR. It indicated that the large concentration aggrandized the chance of touching among effective abrasives and the sapphire. With the larger abrasive

size, the MRR aggrandized first and then declined, manifesting that the aggrandizing of the abrasive size could enhance the contact acreage between the abrasive and the sapphire, but the larger the size the faster the decline in touch. All in all, changing the concentration and particle size of the abrasive can indeed improve the polishing efficiency of the sapphire.

Table 3. The influence of particle size and concentration of abrasive on the polishing efficiency of sapphire.

Abrasive	Size (nm)	Concentration (wt%)	MRR (μm/h)	Conclusion	Ref.
colloid silica	20, 50, 80, 100	20	2.02–3.64	With the increase of size and concentration of abrasive, the sapphire MRRs increase.	[68]
colloid silica	100	0–40	0–4.97		[68]
colloid silica	30, 60, 80, 100, 120, 140	10–30	/		[77]
colloid silica	20–60	0–70	/		[78]
colloid silica	20, 30, 40, 50, 60	/	/		[79]
mixed sol of SiO_2-Al_2O_3	20–30	SiO_2 is 33, Al_2O_3 is 0–2.5	6–11.25		[80]
colloid silica	20, 55	/	0.42, 1.42		[81]
colloid silica	40, 72, 82.5	/	0.36, 0.56, 0.39 at 400 g/cm^3 pressure		[82]
colloid silica	40	6, 20, 40 wt%	0.36, 0.86, 1.23		[82]
silica particle	/	5–40 wt%	0.3–1.38		[83]
colloidal silica	80	2–12 wt%	1.25–2.027		[84]

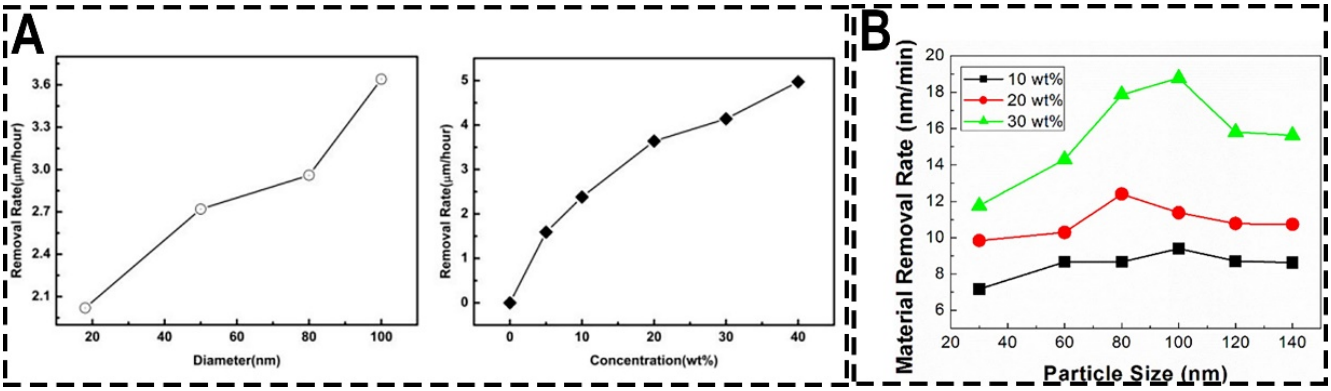


Figure 7. (**A**) MRR variation with changing the particle size and concentration of silica sol [68]. Adapted with permission. Copyright 2018, The Korean Institute of Electrical Engineers. (**B**) MRR of silica-based slurry with different abrasive concentration as a function of mean particle size [77]. Adapted with permission. Copyright 2017, Electrochemical Society.

3.2.3. Changing the Morphology of Abrasive

To enhance the polishing performances of silica sol, many researchers have carried out abundant studies on nonspherical silica [75,85–88]. For instance, Dong et al. synthesized chain-shaped irregular SiO_2 using the chain structure of PEG200 and many oxygen-functional groups [75]. The MRR of irregular silica nanoparticles increased by 58.7% compared to that of spherical silica nanoparticles. In addition, they synthesized potato, chain- and flower-shaped irregular SiO_2 nano abrasiades (ISNAs) using a nickel-ion-induced effect growth method [86]. During the CMP process, the touch acreage between sapphire and ISNAs aggrandized, the solid state reaction aggrandized, and MRR increased by 22.72%. Non-spherical SiO_2 as an abrasive is able to enhance its polishing performance and expand its application potential. Xu et al. used a fresh dual-system microemulsion template means to prepare a single irregular-flower-shaped SiO_2 abrasive to replace the traditional spherical SiO_2 (Figure 8A) [87]. According to CMP tests, under 6% concentration, the MRR of flower-like silica was 217.4% of spherical SiO_2 (Figure 8B). The Ra value was also lower (Figure 8C). The mechanism of the flower-like silica to enhance the buffing

efficiency was that its anomalous morphology enhanced the effective contact with the sapphire (Figure 8D). In summary, the non-spherical SiO_2 has a higher MRR to sapphire than that of traditional spherical SiO_2, because the contact area between non-spherical SiO_2 and sapphire is increased, which leads to more solid-phase chemical reactions between the abrasive and sapphire [87]. There are two disparate synthetic processes for nonspherical silica. The first is to link several spherical SiO_2 into dumbbell or thready-shaped SiO_2; the second is to synthesize individual nonspherical silica particle [85–88]. The former is widely used in the research of improving the CMP of sapphire due to its ease of synthesis, while the individual particle surface morphology of the latter is extremely irregular and the preparation means are complex, which was not put into use.

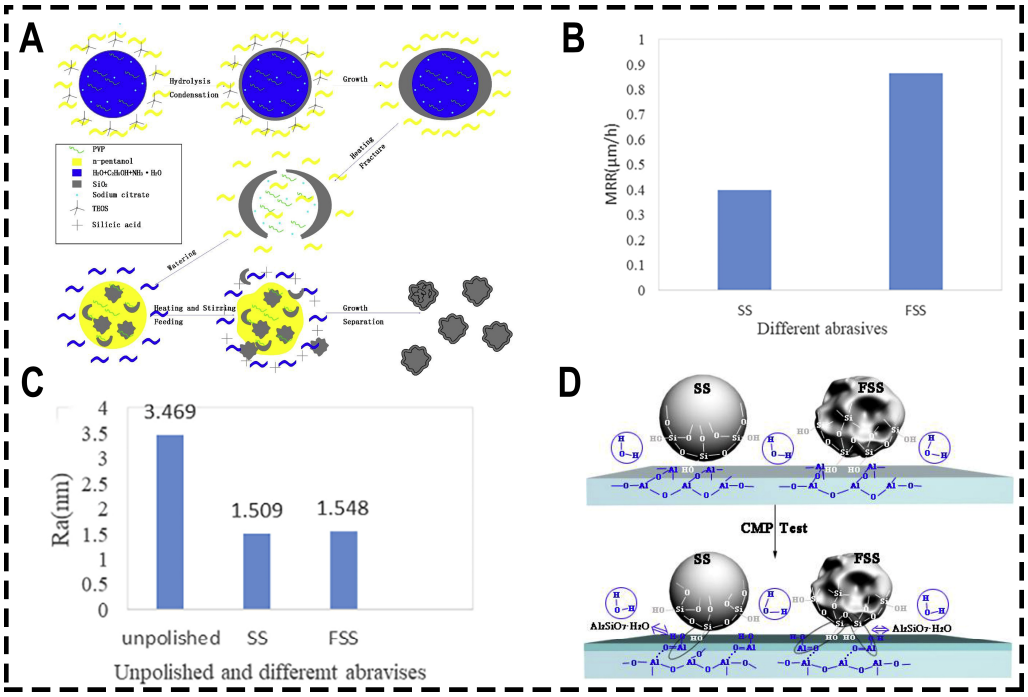


Figure 8. (**A**) Schematic diagram of preparation of floriform silicon abrasive. (**B**) Under 6.0 wt% concentration, the MRR values of SS and FSS abrasives. (**C**) Ra with disparate treatments of sapphire. (**D**) The abrasion mechanism between silica abrasives and sapphire [87]. Adapted with permission. Copyright 2019, Elsevier B.V.

3.2.4. Constructing Composite Abrasives

At the moment, chemical modification of abrasives has been certified to be resultful in enhancing the CMP performance of sapphire [89–109]. Table 4 demonstrates the influence of the composite abrasives on the polishing efficiency of sapphire [89–92,98–100,105]. Typically, in the work of Lei's research group, they doped metal ions such as Co/Fe/Cu/Ni/Zn in SiO_2 to form metal-doped SiO_2 composite abrasives, and found that solid chemical reactions occurred on the surface of sapphire during the grinding process of composite abrasives and sapphire [94–98]. The intermediate layer such as $CoAl_2O/AlFeO_3/Al_2CuO_4/NiAl_2O_4/Al_2ZnO_4$ was formed and was easy to be removed. Under the same conditions, composite abrasives exhibited higher MRR and lower Ra than pure SiO_2 abrasives in CMP of sapphire substrates. In addition to metal ion doping, Zhou et al. constructed a PS@CeO_2/DND compound abrasive [99]. Under the same conditions, the MRR of sapphires polished with compound abrasives were 10%–20% higher than of onefold abrasive. The elevation in CMP efficiency could be put down to the synergistic effect of the active CeO_2 abrasive, the large rigidity of DND, and the large resilience of PS balls. Furthermore, Wang et al. first proposed a novel branched-chain inorganic polyelectrolyte (polymerized ferric aluminum zinc magnesium silicate (PSMFAZ)) as an effective binder to modify colloidal SiO_2, and constructed

a PSMFAZ-SiO_2 composite abrasive (Figure 9A) [100]. When the composite abrasive was used in the CMP of sapphire, due to the adhesion of an inorganic polyelectrolyte to the surface of colloidal SiO_2, the electrostatic repulsion between the particles was reduced, and the contact between the abrasive and sapphire was increased according to the Al XPS (Figure 9B). Therefore, the soft layer formed by the chemical reaction could be quickly removed, and the chemical–mechanical collaborative process was optimized, thus obtaining a higher MRR (Figure 9C). The results showed that the MRR of the sapphire wafer was increased by 23.76% compared with pure silica sol (Figure 9D). Furthermore, Wang et al. prepared Al_2O_3-SiO_2 core–shell nanoparticles, and then coated polyelectrolyte (PSMAZ) on the surface using electrostatic adsorption to obtain a PSMAZ-Al_2O_3/SiO_2-composite abrasive [101]. Due to the good dispersion of composite abrasives, which accelerated the mechanical removal process in sapphire CMP, the MRR of composite abrasives was 30% higher than that of pure Al_2O_3 abrasives. All in all, the modification of abrasive particles mainly includes metal ion doping, the construction of binary or ternary composite abrasives, polymer adhesion, and so on. Compared with a single abrasive, the composite abrasive has a higher MRR and lower Ra for sapphire.

Table 4. The influence of the composite abrasives on the polishing efficiency of sapphire.

Composite Abrasives	The Changing Trend of MRR	The Changing Trend of Ra	Conclusion	Ref.
Ag-doped colloidal silica	MRR increases with the increase of Ag^+ doping amount	With increase of Ag^+ doping amount, Ra decreases first, reaches the minimum, and then increases	In the polishing process, the doping of metal ions can accelerate the solid-state reaction between the abrasive and the sapphire, thereby increasing the MRR and reducing the Ra of sapphire	[89]
Sm-doped colloidal silica	MRR increases with the increase of Sm^{3+} doping amount	With increase of Sm^{3+} doping amount, Ra decreases first, reaches the minimum, and then increases		[90]
CeO_2-doped colloidal SiO_2	MRR increases with the increase of CeO_2 doping amount	Ra decreases with increase of CeO_2 doping amount		[91]
Ti-doped colloidal SiO_2	MRR increases with the increase of Ti doping amount	Ra decreases with increase of Ti doping amount		[92]
Zn-doped colloidal SiO_2	With increase of $Zn(OH)_2$ doping amount, MRR increases first, reaches the maximum, and then decreases	With increase of $Zn(OH)_2$ doping amount, Ra decreases first, reaches the minimum, and then increases		[98]
PS@CeO_2/DND	MRR for PS@CeO_2, PS@DND and PS@CeO_2/DND reached 1.2, 1.6 and 1.7 μm/h, respectively	Ra for PS@CeO_2, PS@DND and PS@CeO_2/DND reached 1.25, 0.63 and 0.52 nm, respectively	Under the combined action of super hard diamond particles, chemically active abrasive CeO_2 and elastic PS balls, PS@CeO_2/DND has good CMP performance	[99]
PSMFAZ-SiO_2	With increase of PSMFAZ doping amount, MRR increases first, reaches the maximum, and then decreases	With increase of PSMFAZ doping amount, Ra decreases first, reaches the minimum, and then increases	The addition of PSMFAZ reduces the electrostatic repulsion between particles and increases the contact between sapphire and abrasive, thus obtaining a higher MRR	[100]
γ-Al_2O_3/SiO_2	With increase of SiO_2 doping amount, MRR increases first, reaches the maximum, and then decreases	With increase of SiO_2 doping amount, Ra decreases first, reaches the minimum, and then increases	After the introduction of silica, the hydration of gamma-alumina is prevented, and the removal amount is increased	[105]

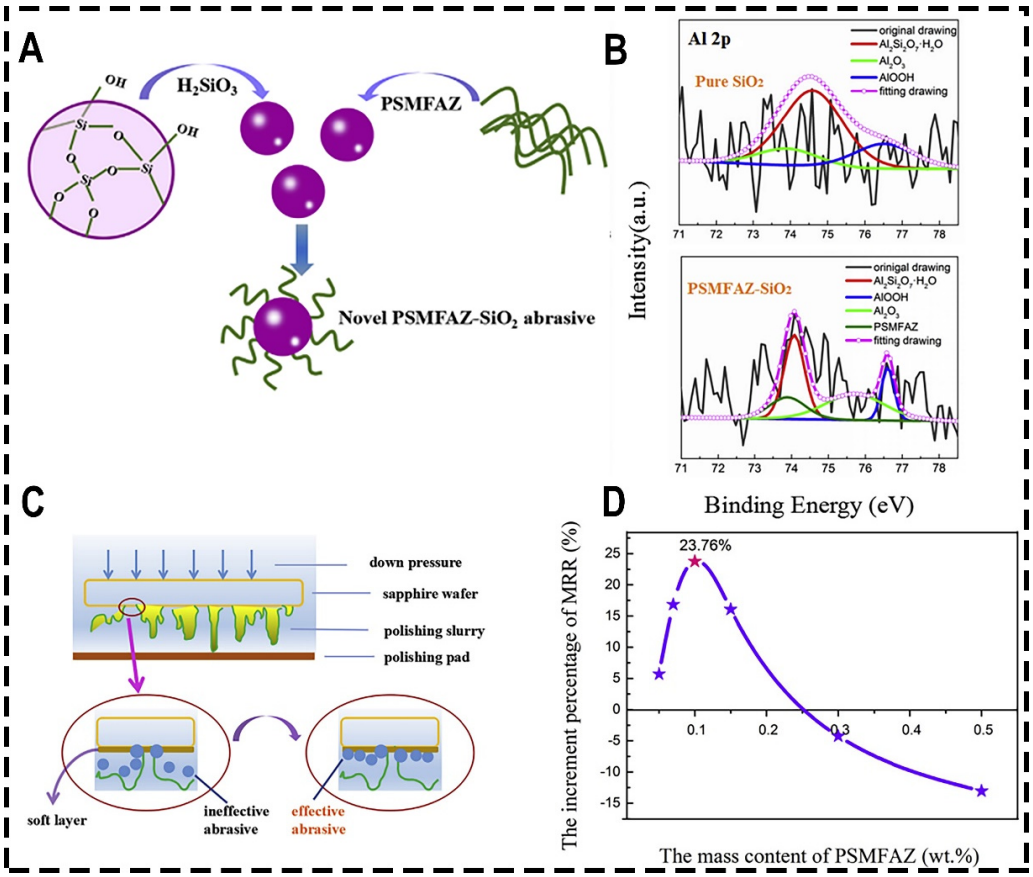


Figure 9. (**A**) Schematic diagram of the synthesis of polyelectrolyte (PSMFAZ)-SiO_2 abrasive. (**B**) The Al 2p XPS spectra in PSMFAZ-SiO_2 abrasive after polishing. (**C**) Contact diagram of PSMFAZ-SiO_2 abrasive and sapphire. (**D**) Contrasted with no PSMFAZ polishing slurry, and the changing of MRR with PSMFAZ concentration in abrasive [100]. Adapted with permission. Copyright 2019, Elsevier B.V.

3.2.5. Changing the pH of the Slurry

The pH value of the slurry also markedly affects the MRR and Ra of sapphire in the CMP course. In general, when the pH of the slurry changes, the zeta potential and size of the abrasive will change. The formation trend of the hydration reaction layer also changes with pH value. It is well known that nitric acid (HNO_3), potassium hydroxide (KOH), sodium hydroxide (NaOH), and strontium hydroxide ($Sr(OH)_2$) are often used as inorganic alkaline pH regulators [77,110–113]. The FA/O chelating agent, aminopropanol (AMP) and sodium metasilicate (SMSN) are organic base pH regulators [114,115]. As we all know, Al_2O_3 is an amphoteric oxide that will react with acids or bases. However, sapphire is a kind of ceramic Al_2O_3, which is not easy to etch using acid and alkali, so the reaction between acid or alkali and sapphire is very sluggish [116]. The acid or base reaction is shown in Equations (10)–(15). Under acidic conditions, the surface of sapphire is positively charged and covered by Al^{3+} and Al-OH species. Under alkaline conditions, the surface is negatively charged and covered with Al-OH and AlO_2^- species. Generally speaking, the acid polishing is easy to cause corrosion and damage to the equipment, so alkaline polishing is generally prepared with an alkaline pH regulator.

$$Al_2O_3 + 6H^+ = 2Al^{3+} + 3H_2O \quad (10)$$

$$Al(OH)_3 + 3H^+ = Al^{3+} + 3H_2O \quad (11)$$

$$AlO(OH) + 3H^+ = Al^{3+} + 2H_2O \quad (12)$$

$$Al_2O_3 + 2OH^- = 2AlO_2^- + H_2O \quad (13)$$

$$Al(OH)_3 + OH^- = AlO_2^- + 2H_2O \quad (14)$$

$$AlO(OH) + OH^- = AlO_2^- + 2H_2O \quad (15)$$

Table 5 summarizes the effect of a pH regulator on the polishing efficiency of sapphire [110–114]. For instance, Yin et al. used $Sr(OH)_2$ to adjust the pH value of the polishing solution [113]. According to XPS and XRD data, compared with the traditional KOH pH regulator, $Sr(OH)_2$ could promote the break of Al-O-Al chemical bonds in sapphire, and form $SrAl_2Si_2O_8$ and $SrAl_2O_4$ interlayers that could be easily removed (Figure 10A,B). As a result, the MRR of sapphire was higher when the pH regulator is $Sr(OH)_2$ (Figure 10C,D). Wang et al. mixed macromolecular FA/O chelating agents with KOH as a novel pH regulator [114]. Figure 10E uncovered that the MRR of sapphire was first enhanced and then declined with the increase of the mixed base volume, and Ra changed in reverse situation. Because the atomic structures of c-plane and r-plane sapphires were disparate, the difficulty and thickness of the hydrated layer form on sapphire were disparate. Under the same conditions, the MRR of c-plane and r-plane sapphires were 3.23 μm h^{-1} and 0.607 μm h^{-1}, respectively, and the Ra were 0.226 nm and 0.309 nm, respectively (Figure 10F,G).

Table 5. The effect of pH regulator on the polishing efficiency of sapphire.

pH Conditioning Agent	The Changing Trend of MRR	The Changing Trend of Ra	Conclusion	Ref.
KOH, HNO_3	As the pH increases, from acidic to basic, the MRR gradually increases until it is saturated	Ra has barely changed	When pH changes, the MRR of sapphire is mainly affected by the change of Zeta potential of abrasive and hydration layer formed in sapphire. Due to electrostatic attraction, more abrasives are involved in the polishing process under acidic conditions, which increases the MRR under acidic conditions. Under alkaline conditions, the surface of sapphire is more likely to form a hydration layer, so the MRR of sapphire under alkaline conditions is higher	[110]
KOH	Under basic conditions, MRR increased with the increase of pH value	Ra decreases with increase of pH value	The higher the pH value, the thicker the hydration layer formed on the sapphire surface, and the faster the sapphire removal rate	[112]
$Sr(OH)_2$	With increase of pH value, MRR increases first, reaches the maximum, and then decreases	/	$Sr(OH)_2$ can not only condition the pH of the polishing liquid, but also hydrate with the sapphire, promoting the chemical reaction between the slurry and the sapphire substrate	[113]
FA/O and KOH	When the volume ratio of FA/O to KOH is 1:20, the MRR is the highest	When the volume ratio of FA/O to KOH is 1:20, the Ra is the lowest	When the mixed base of the organic base and KOH is used as a pH regulator, the strong base can maintain the alkaline environment, enhance the stability of the slurry, the organic base can precipitate OH^- precipitate, and the reaction product can be removed in time, resulting in the reduction of MRR	[114]

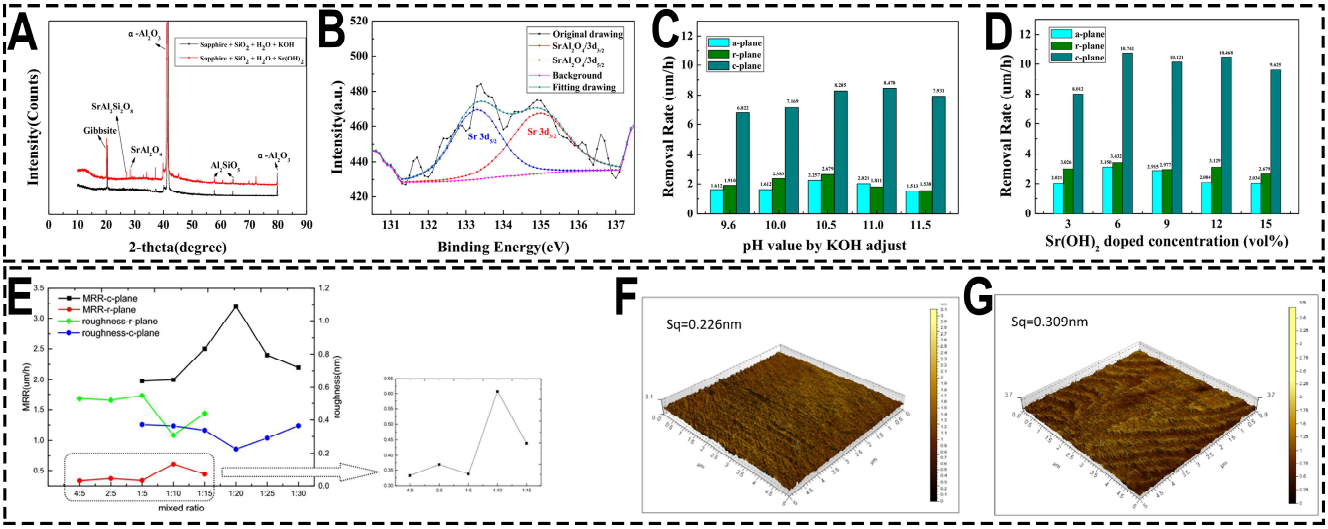


Figure 10. (**A**) XRD analysis of polished sapphire with unblended and blended $Sr(OH)_2$ fluid. (**B**) XPS analysis of element Sr after polishing using $Sr(OH)_2$ blended fluid. The influence of the pH value regulated by KOH (**C**) and $Sr(OH)_2$ (**D**) to the MRR of sapphire in a/r/c plane [113]. Adapted with permission. Copyright 2019, Electrochemical Society. (**E**) When the pH was 10, the variation of MRR and Ra with the volume ratio of mixed alkali. Ra of c-plane (**F**) and r-plane (**G**) sapphires with mixed base volume ratios of 1:20 and 1:10, respectively [114]. Adapted with permission. Copyright 2017, Electrochemical Society.

3.2.6. Changing the Complexing Agent

In CMP, material removal is achieved through a combination of chemical and mechanical actions. On various occasions, if the removable substance cannot be taken away from sapphire in time, it will adhere to the surface of sapphire, thus affecting its buffing quality. Complexing agents can trap residual metal cations on the surface of sapphire wafers and carry the ions away from the polished surface in the form of soluble complexes. Complexing agents are key chemical components in CMP slurry. At present, the main CMP complexing agents are sorbitol, triethanolamine (TEA), sodium gluconate (Gluc), ethylenediamine tetraacetic acid (EDTA), 1, 2-dimethyl-3-hydroxy-4-pyridine (DHPO), and other compounds with hydroxyl or carboxyl groups [62,117–122]. Table 6 shows the effect of the complexing agent on the polishing efficiency of sapphire [117–120]. For example, Xie et al. developed the environmentally friendly polishing slurry using sorbitol or TEA as coordination agents to solve the hazards of traditional additives to operators and the environment [62]. The chelating agent in the polishing slurry chelated with $Al(OH)_4^-$ ions on the sapphire surface to form a soluble complex, which increased the removal of $Al(OH)_4^-$ ions. Qu et al. investigated the effect of the hydroxy–carboxylate complexing agent on m-plane sapphire CMP [118]. As shown in Figure 11A, during the polishing procedure, $Al(OH)_4^-$ ions were formed on the sapphire surface, which would be chelated with sodium gluconate(Gluc) to shape the $Al(OH)_4^-/Gluc^-$ chelate. This chelate was solvable and easily wiped off with abrasives, thus enhancing the MRR of the sapphire. As a consequence, the MRR of the m-plane sapphire was elevated to 5.358 μm h^{-1}, which was 50% lager than that of the baseline fluid, and the surface root-mean-square roughness was minished to 0.172 nm (Figure 11B,C). Zhang et al. investigated the influence of different complexing agents, namely sodium oxalate ($Na_2C_2O_4$), aminotriacetic acid (NTA), ethylenediamine tetraacetic acid disodium (EDTA-2Na), and diethyl triamine pentaacetic acid (DTPA) on alumina slurry in sapphire CMP [119]. It was assumed that the carboxyl group in the complexing agent could be complexed with the surface of Al_2O_3 to form a C-O-Al bond, which increased the spatial resistance between molecules and improved the dispersion of Al_2O_3 (Figure 11D). When the number of carboxyl groups in the molecule increased to four or more, there were still redundant active sites. During the polishing process, this additional

active site might be complexed with $Al(OH)_3$ on the sapphire surface to form a softened C-O-Al structure, which was more easily removed using Al_2O_3 particles in the polishing slurry during the polishing process. However, when the number of carboxyl groups in the complexer molecule was increased to five (DTPA), a DTPA molecule could be complexed with several Al_2O_3 particles, resulting in a higher attraction than the steric resistance. In theory, the larger the molecular weight, the longer the molecular chain formed, and the stronger the spatial resistance and even bending and winding, resulting in agglomeration between particles, further resulting in a decline in polishing rate. The results showed that with the increase of the carboxyl group number in the complexing agent, the MRR of sapphire increased first and then decreased (Figure 11E). When the complexing agent was EDTA-2Na (carboxyl group number is four), the removal rate of the sapphire could reach about 4.0 μm/h, which was 52% higher than that without the complexing agent, and the surface roughness of the sapphire was 0.96 nm, which was 51% lower than that without the complexing agent (Figure 11F).

Table 6. The effect of a complexing agent on the polishing efficiency of a sapphire.

Complexing Agent	The Changing Trend of MRR	Conclusion	Ref.
Sorbitol	/	The $Al(OH)_4^-$ ions formed on the sapphire surface chelate with the chelating agent to form chelates. Chelates are soluble and easily removed from the sapphire surface by abrasives, so the MRR of a sapphire can be increased	[117]
PT, Cit, Gluc	With the addition of PT, Cit, and Gluc, MRR increases first and then decreases		[118]
NaAc, $Na_2C_2O_4$, NTA, EDTA-2Na, and DTPA	MRR first increased and then decreased with the increase of carboxylic acid in the complex agent		[119]
Chitosan oligosaccharide	With the increase of chitosan oligosaccharide doping amount, MRR increases first, reaches the maximum, and then decreases		[120]

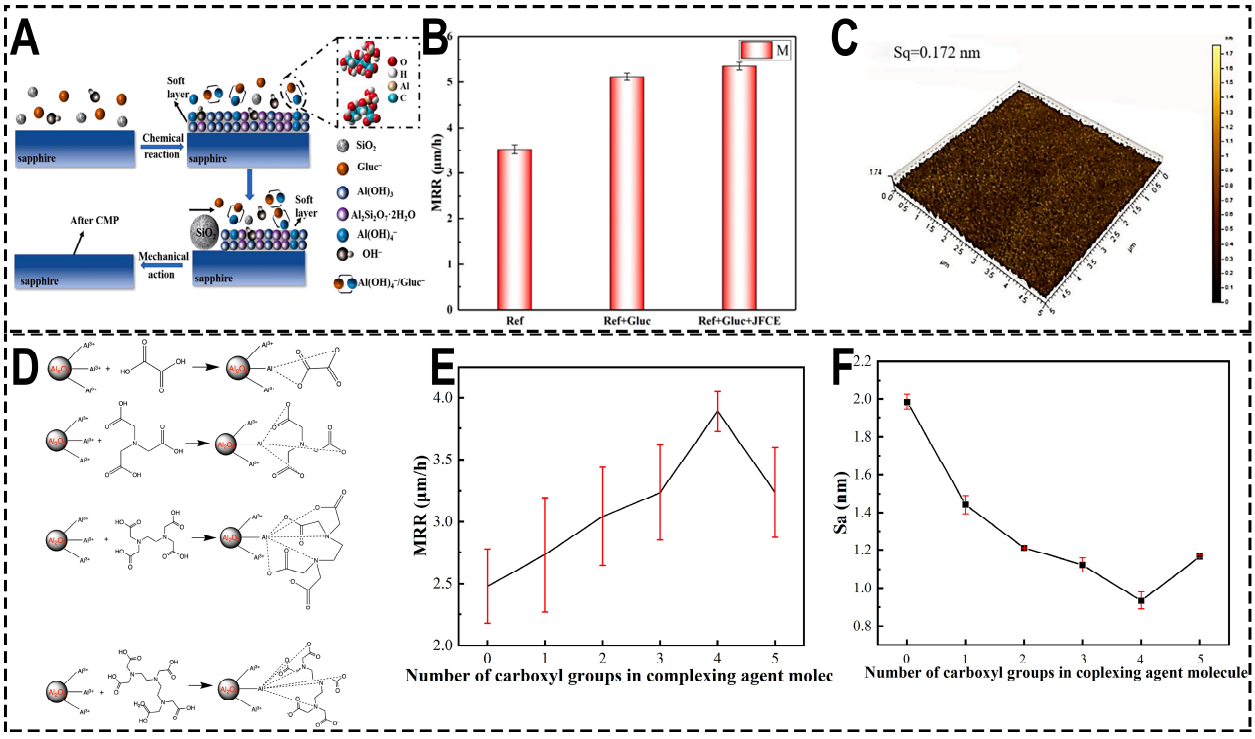


Figure 11. (**A**) Removal-mechanism diagram of M-plane sapphire CMP. (**B**) Removal-mechanism diagram of M-plane sapphire CMP. (**C**) the surface roughness of slurry polished wafers after optimization [118]. Adapted with permission. Copyright 2023, Elsevier B.V. (**D**) chelating formulas

between complexing agents and Al_2O_3 particles: $Na_2C_2O_4$, NTA, EDTA-2Na, and DTPA, respectively. MRR (**E**) and Sa (**F**) changes with the number of carboxyl groups in the complex agent [119]. Adapted with permission. Copyright 2023, Elsevier B.V.

3.2.7. Other Additives

In addition to the above abrasive, complexing agents and pH regulators, and other components of the polishing slurry such as surfactants, oxidants, catalysts, etc., will also impact the MRR and Ra of sapphire [77,123–132]. For instance, surfactants have multiple properties such as adhesion and osmosis, which can dramatically alter the interface properties of the solution. For instance, as demonstrated in Figure 12A, Zhao et al. added anionic surfactants to the fluid to wrap silica sol, so that particles appear in the mutually exclusive state rather than gathering [126]. Meanwhile, surfactants also had a tutelar effect on the depression of sapphire. The experimental results demonstrated that the MRR of the sapphire was influenced by the amount of surfactant (Figure 12B). Zhang et al. researched the effect of the type of metal salt on sapphire CMP [77]. As shown in Figure 12C,D, in addition to fluoride, most alkali metal salts and halides could be used as polishing accelerators to improve the MRR of sapphire, because the double electric layer of colloidal silica particles could be densified with enhanced ion concentration in the fluid, and, consequently, abrasives gathered. Hence, within a particular concentration scope, the MRR enhanced with the increase of metal salt concentration. However, when the concentration of metal salt was too large, the abrasive accumulation was too serious and the MRR would decline. Lu et al. added $K_2S_2O_8$ catalyst in the polishing fluid, which could react with a sapphire surface to elevate the polishing effect of sapphire. The consequences manifested that the MRR of c-, a-, and r-plane sapphire were as high as 8.235 μm h^{-1}, 3.314 μm h^{-1}, and 3.053 μm h^{-1}, respectively [130]. Xu et al. found that when non-precious metal material Fe-N_X/C was used as a catalyst, the MRR of sapphire during the CMP process in SiO_2-based polishing slurry could be increased by 15.44% (Figure 12E) [131]. On the basis of the above, they also developed a new iron-based catalyst $SoFe^{III}$, which significantly improved the removal rate of sapphire, with a removal rate of 7.21 μm/h, which was 1.66 times the removal rate of catalyst-free paste (Figure 12F) [132].

3.3. Introducing Other Polishing Processes

Although researchers have continuously elevated the machining efficiency and surface quality of sapphire by improving the polishing-process parameters or the composition of the polishing slurry, the time cost is still very high, and the surface quality is difficult to improve. Therefore, the development of new sapphire-polishing technology is still a top priority. At present, many researchers are exploring how to introduce new processes into sapphire CMP to improve the CMP efficiency of sapphire. Among them, ultrasonic (UV)-assisted CMP is currently the most commonly used technology to assist in improving sapphire CMP [133–137]. For instance, Xu et al. employed conventional CMP and an ultrasonic bending vibration (UFV) assisted CMP (UFV-CMP) to polish sapphire substrates under different pressures, respectively (Figure 13A) [134]. UFV-CMP endowed traditional CMP equipment with ultrasonic processing functions. The MRR of UFV-CMP was twice as large as that of traditional CMP. The surface roughness of the polished sapphire substrate of UFV-CMP is 0.83 Å. Zhou et al. proposed a novel model of MRR to explore the mechanism of sapphire UA-CMP [137]. It contained two modes, namely two-body wear and abrasive impact. The experiments manifested that when the revolving speed elevated from 40 to 80 r min^{-1}, the MRR elevated by about 63%. The Ra after polishing was declined from 0.10 nm to 0.07 nm. Xu et al. used gas–liquid-assisted chemical–mechanical polishing (GLA-CMP) instead of traditional CMP to improve the surface polishing efficiency of sapphire wafers (Figure 13B) [35]. The experimental results showed that the removal rate of sapphire by the GLA-CMP process was 77.6 nm min^{-1}, which was 10.23% higher than that using the traditional CMP process. Under normal circumstances, what we call CMP refers to the single-sided CMP, that is, only one side of the sapphire is polished. However,

single-sided CMP usually has the problem of a low polishing rate, so some researchers have proposed the introduction of double-sided CMP into the sapphire CMP process, and it has been proved that the working efficiency of double-sided CMP is higher than that of single-sided CMP [138,139]. For instance, Li et al. explored the working efficiency of dual-sided CMP of sapphire, and the results showed that the MRR and Ra of dual-sided sapphire CMP were significantly superior to that of single-sided CMP under the same parameters (Figure 13C) [139]. Compared with single-sided CMP, the MRR of dual-sided sapphire CMP was improved by 14.016 nm/min, and better surface quality could also be obtained under higher polishing pressures.

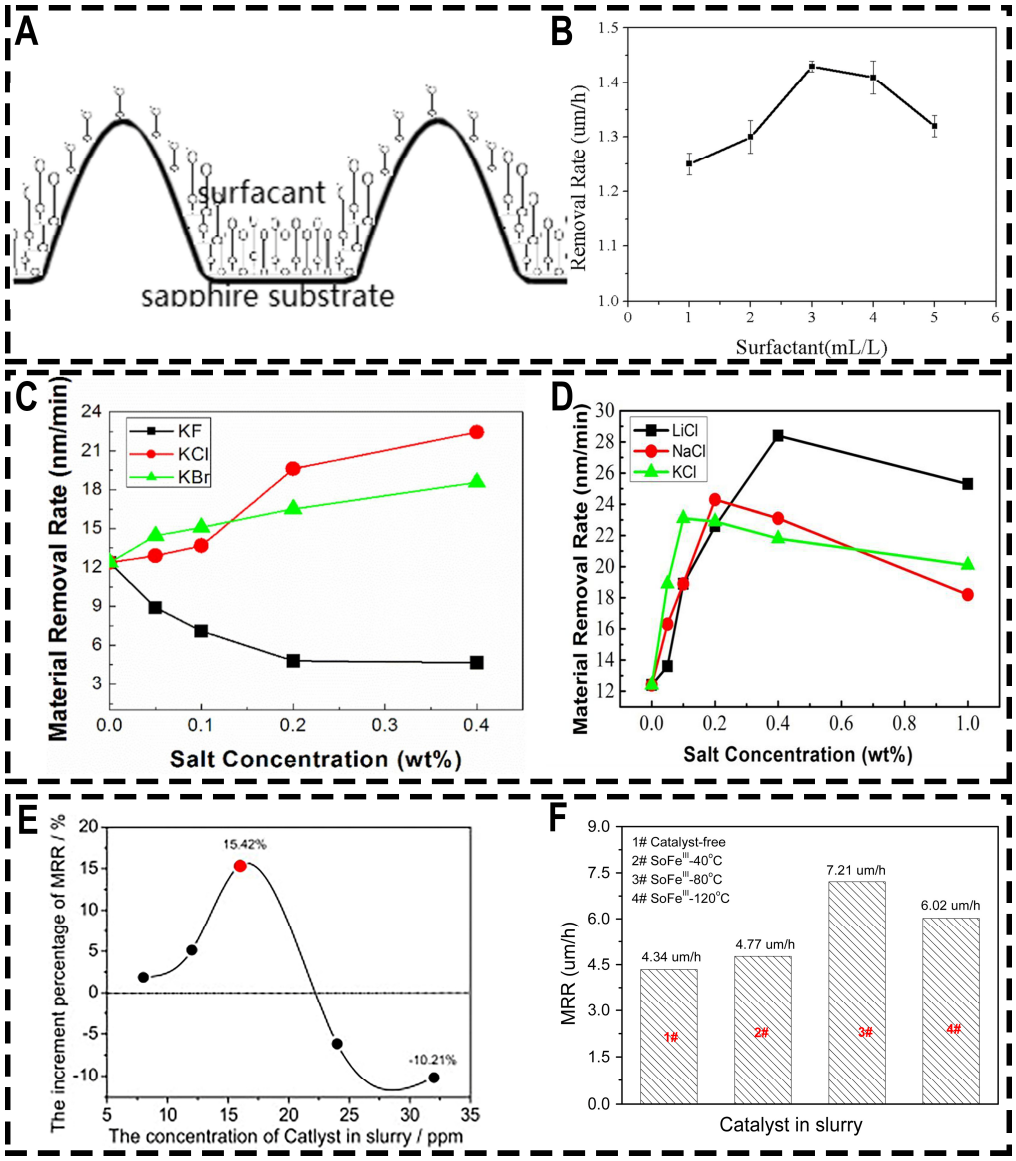


Figure 12. (**A**) Surfactant distribution on sapphire surface. (**B**) Relation between MRR of r-plane sapphire and surfactant concentration [126]. Adapted with permission. Copyright 2018, Electrochemical Society. (**C**) Relation between MRR of sapphire and concentration variations of three halogen salts. (**D**) The variation of sapphire MRR with the concentration of metal salt [77]. Adapted with permission. Copyright 2017, Electrochemical Society. (**E**) Dependence of the sapphire removal rate on the Fe-Nx/C concentration in the suspension (unit: %, compared with the MRR using catalyst-free polishing slurry) [131]. Adapted with permission. Copyright 2015, Elsevier B.V. (**F**) Sapphire MRR with catalyst drying at different temperature [132]. Adapted with permission. Copyright 2018, Elsevier B.V.

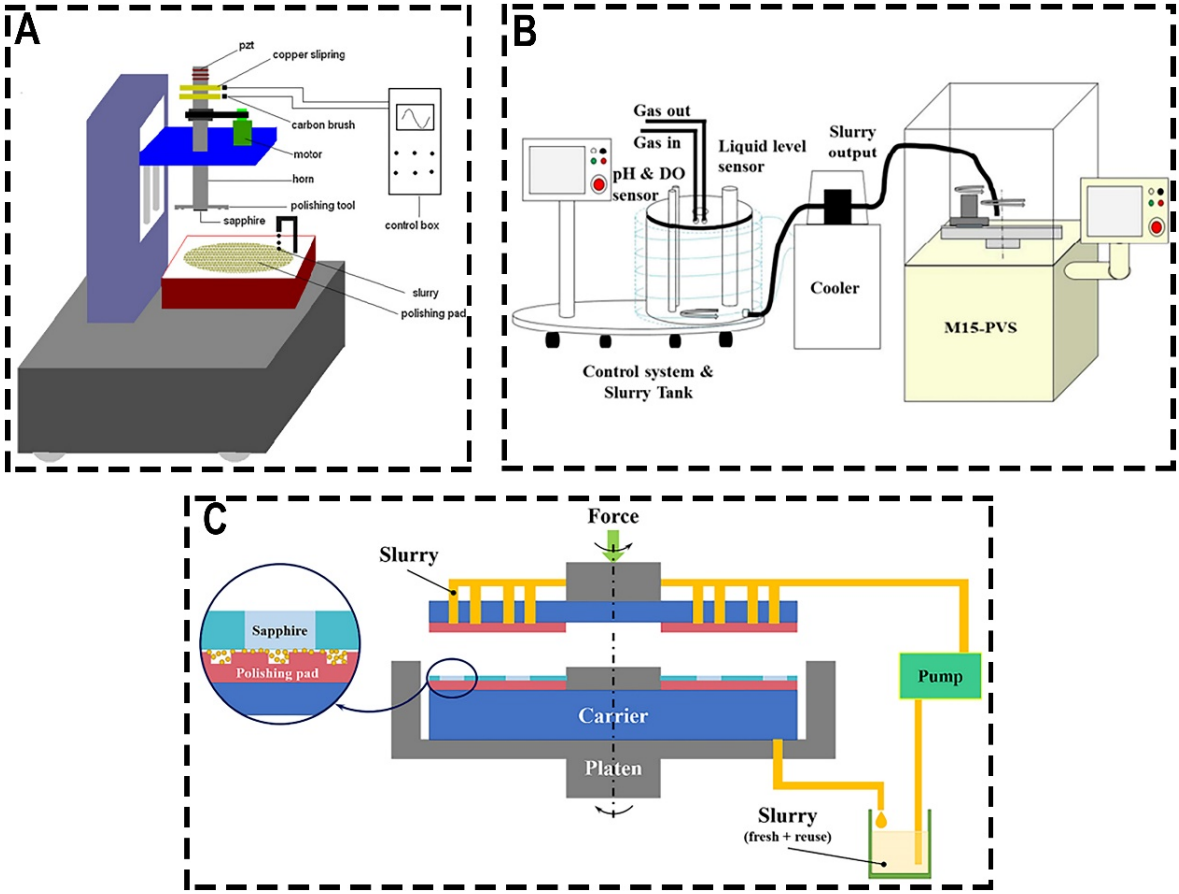


Figure 13. (**A**) Schematic of UFV–CMP system [134]. Adapted with permission. Copyright 2023, Springer Nature. (**B**) Illustration of GLA-CMP apparatus [35]. Adapted with permission. Copyright 2018, Elsevier B.V. (**C**) Schematic diagram of double-sided CMP machine [139]. Copyright 2022, Springer Nature.

4. Summary and Outlook

As shown in this review, the research and application of sapphire CMP has shown a booming trend with the passage of time. Owing to the rapid development of semiconductor technology, higher requirements are being put forward for the machining efficiency and surface quality of sapphire. For example, the sapphire used for the LED substrate requires its surface roughness to be between 0.2–0.5 nm after polishing [34]. However, it is still a tremendous challenge to obtain a satisfactory chemical–mechanical polishing result in view of the significant rigidity, brittleness, and chemical inertness of sapphire. This paper reviews the recent research progress of sapphire CMP, including the mechanism of sapphire CMP, and how to elevate the efficiency of sapphire CMP. According to the composition of the sapphire CMP polishing system, the processing efficiency and surface quality of sapphire CMP can be improved for both the mechanical and chemical aspects. For the mechanical aspect, it is necessary to improve the polishing process, such as by optimizing the polishing pressure and polishing speed. For the chemical aspect, it is necessary to optimize the composition of the polishing liquid. For instance, changing the hardness, size, and morphology of abrasives, constructing composite abrasives, changing the pH value of polishing slurry, changing the complexing agent of polishing slurry, adding other additives, and introducing new polishing auxiliary processes, such as ultrasonic-assisted polishing or gas–liquid-assisted polishing process. We expect that the findings of this review will drive the further development of sapphire CMP. To better develop advanced sapphire CMP processes, the following pressing issues must be considered:

1. The change of polishing parameters will influence the polishing efficiency of sapphire CMP, but the mechanism by how polishing parameters affect the effect of sapphire CMP is still controversial.
2. The deep mechanism of the influence of abrasive hardness, and particle size and concentration on sapphire CMP has not been fully explored, and the interaction mechanism between the abrasive and sapphire is still controversial.
3. The mechanism of interaction between other components such as surfactants, oxidants, and chelating agents in the polishing fluid and sapphire needs to be further explored. Only in this way, we can clearly understand the role of each component in the sapphire CMP, and better configure the polishing slurry.
4. New and simple polishing supplementary means should be introduced into the CMP process of sapphire to improve the polishing efficiency and polishing quality of sapphire.

In summary, based on in-depth research and the emergence of higher demand, sapphire CMP has received more and more attention in the literature. However, we still have many challenges to resolve. We hope that the literature review on the progress of the sapphire CMP process will be helpful to the further development of the sapphire CMP process in the future.

Author Contributions: Conceptualization, S.L., Z.H. and S.W.; investigation, S.L. and J.F.; writing, S.L. and Y.L. All authors have read and agreed to the published version of the manuscript.

Funding: This work was jointly supported by the National Key Research and Development Plan Project (green and efficient utilization of middle- and low-grade silica-calcareous collophosphates and coupled preparation of high-quality phosphating products technology (No. 2022YFC2904700)).

Data Availability Statement: Data are contained within the article.

Conflicts of Interest: Authors Shaoping Li, Zhaobo He and Yue Luo were employed by the company Hubei Sinophorus Electronic Materials Co., Ltd. The remaining authors declare that the research was conducted in the absence of any commercial or financial relationships that could be construed as a potential conflict of interest.

References

1. Gong, Z. Layer-scale and chip-scale transfer techniques for functional devices and systems: A review. *Nanomaterials* **2021**, *11*, 842. [CrossRef] [PubMed]
2. Hao, Y.; Xiang, S.; Han, G.; Zhang, J.; Ma, X.; Zhu, Z.; Guo, X.; Zhang, Y.; Han, Y.; Song, Z.; et al. Recent progress of integrated circuits and optoelectronic chips. *Sci. China Inf. Sci.* **2021**, *64*, 201401. [CrossRef]
3. Juska, V.B.; Maxwell, G.; Estrela, P.; Pemble, M.E.; O'Riordan, A. Silicon microfabrication technologies for biology integrated advance devices and interfaces. *Biosens. Bioelectron.* **2023**, *237*, 115503. [CrossRef] [PubMed]
4. Shahbaz, M.; Butt, M.A.; Piramidowicz, R. Breakthrough in silicon photonics technology in telecommunications, biosensing, and gas sensing. *Micromachines* **2023**, *14*, 1637. [CrossRef]
5. Fujii, T.; Hiraki, T.; Aihara, T.; Nishi, H.; Takeda, K.; Sato, T.; Kakitsuka, T.; Tsuchizawa, T.; Matsuo, S. Development of an epitaxial growth technique using III-V on a Si platform for heterogeneous integration of membrane photonic devices on Si. *Appl. Sci.* **2021**, *11*, 1801. [CrossRef]
6. Li, K.H.; Fu, W.Y.; Choi, H.W. Chip-scale GaN integration. *Prog. Quantum Electron.* **2020**, *70*, 100247. [CrossRef]
7. Iyengar, S.A.; Bhattacharyya, S.; Roy, S.; Glavin, N.R.; Roy, A.K.; Ajayan, P.M. A researcher's perspective on unconventional lab-to-fab for 2D semiconductor devices. *ACS Nano* **2023**, *17*, 12955–12970. [CrossRef]
8. Zhang, Z.; Xiao, Y.; Wang, J.; Miao, P.; Liu, H.; Cheng, Y.; Gou, Y.; Wang, S.; Deng, G.; Zhou, S. High-power and low-threshold 1200 nm InGaAs/GaAs quantum-wells VECSEL grown by MOCVD. *J. Lumin.* **2023**, *263*, 120022. [CrossRef]
9. Gao, Z.; Ju, X.; Zhang, H.; Liu, X.; Chen, H.; Li, W.; Zhang, H.; Liang, L.; Cao, H. InP quantum dots tailored oxide thin film phototransistorfor bioinspired visual adaptation. *Adv. Funct. Mater.* **2023**, 2305959. [CrossRef]
10. Wang, Y.; Ding, Y.; Yin, Y. Reliability of wide band gap power electronic semiconductor and packaging: A review. *Energies* **2022**, *15*, 6670. [CrossRef]
11. Li, G.; Wang, W.; Yang, W.; Lin, Y.; Wang, H.; Lin, Z.; Zhou, S. GaN-based light-emitting diodes on various substrates: A critical review. *Rep. Prog. Phys.* **2016**, *79*, 056501. [CrossRef] [PubMed]
12. Cho, J.; Park, J.H.; Kim, J.K.; Schubert, E.F. White light-emitting diodes: History, progress, and future. *Laser Photonics Rev.* **2017**, *11*, 1600147. [CrossRef]

13. Lin, J.; Jiang, F.; Wen, Q.; Wu, Y.; Lu, J.; Tian, Z.; Wang, N. Deformation anisotropy of nano-scratching on C-plane of sapphire: A molecular dynamics study and experiment. *Appl. Surf. Sci.* **2021**, *546*, 149091. [CrossRef]
14. Ham, D.; Oh, S.; Kang, H.C. Competing phases in epitaxial SnO_2 thin films deposited on sapphire (0001) substrates using radio-frequency powder sputtering. *Ceram. Int.* **2022**, *48*, 28396–28403. [CrossRef]
15. Luo, Q.; Lu, J.; Xu, X.; Jiang, F. Removal mechanism of sapphire substrates (0001, 1120 and 1010) in mechanical planarization machining. *Ceram. Int.* **2017**, *43*, 16178–16184. [CrossRef]
16. Song, J.; Choi, J.; Xiong, K.; Xie, Y.; Cha, J.J.; Han, J. Semipolar (2021) GaN and InGaN light-emitting diodes grown on sapphire. *ACS Appl. Mater. Interfaces* **2017**, *9*, 14088–14092. [CrossRef] [PubMed]
17. Armitage, R.; Hirayama, H. M-plane GaN grown on m-sapphire by metalorganic vapor phase epitaxy. *Appl. Phys. Lett.* **2008**, *92*, 092121. [CrossRef]
18. Rajabi, K.; Wang, J.; Jin, J.; Xing, Y.; Wang, L.; Han, Y.; Sun, C.; Hao, Z.; Luo, Y.; Qian, K.; et al. Improving modulation bandwidth of c-plane GaN-based light-emitting diodes by an ultra-thin quantum wells design. *Opt. Express* **2018**, *26*, 24985–24991. [CrossRef]
19. Zhao, D.Q.; Xu, F.; Wang, G.G.; Zhang, S.Y.; Qin, G.S.; Wang, B.L.; Han, J.C. SiO_2/HfO_2 laser film with enhanced protection and antireflection for sapphire infrared windows at high temperatures. *ACS Appl. Electron. Mater.* **2021**, *3*, 4611–4617. [CrossRef]
20. Wang, W.; Yang, W.; Wang, H.; Zhu, Y.; Yang, M.; Gao, J.; Li, G. A comparative study on the properties of c-plane and a-plane GaN epitaxial films grown on sapphire substrates by pulsed laser deposition. *Vacuum* **2016**, *128*, 158–165. [CrossRef]
21. Xu, M.; Xue, Z.; Wang, J.; Zhao, Y.; Duan, Y.; Zhu, G.; Yu, L.; Xu, J.; Wang, J.; Shi, Y.; et al. Heteroepitaxial writing of silicon-on-sapphire nanowires. *Nano Lett.* **2016**, *16*, 7317–7324. [CrossRef] [PubMed]
22. Chen, H.; Buric, M.; Ohodnicki, P.R.; Nakano, J.; Liu, B.; Chorpening, B.T. Review and perspective: Sapphire optical fiber cladding development for harsh environment sensing. *Appl. Phys. Rev.* **2018**, *5*, 011102. [CrossRef]
23. Gong, S.; Zhu, X.; Sun, Y.; Tang, B.; Su, Z. Experimental research on surface characteristics and subsurface damage behavior of monocrystal sapphire induced by helical micro abrasive tools. *Ceram. Int.* **2022**, *48*, 21459–21472. [CrossRef]
24. Yu, Y.; Zhu, W.; Ma, Y.; Song, X.; Zou, H.; Zu, G.; Han, Y.; Ran, X. Novel design of sapphire/spinel transparent ceramic joints with double glass interlayers by coating and bonding. *Ceram. Int.* **2024**, *50*, 1591–1600.
25. De Vargas-Sansalvador, I.M.P.; Fay, C.; Phelan, T.; Fernández-Ramos, M.D.; Capitán-Vallvey, L.F.; Diamond, D.; Benito-Lopez, F. A new light emitting diode-light emitting diode portable carbon dioxide gas sensor based on an interchangeable membrane system for industrial applications. *Anal. Chim. Acta* **2011**, *699*, 216–222. [CrossRef] [PubMed]
26. Katyba, G.M.; Zaytsev, K.I.; Dolganova, I.N.; Shikunova, I.A.; Chernomyrdin, N.V.; Yurchenko, S.O.; Komandin, G.A.; Reshetov, I.V.; Nesvizhevsky, V.V.; Kurlov, V.N. Sapphire shaped crystals for waveguiding, sensing and exposure applications. *Prog. Cryst. Growth Charact. Mater.* **2018**, *64*, 133–151. [CrossRef]
27. Fu, J.H.; Min, J.; Chang, C.K.; Tseng, C.C.; Wang, Q.; Sugisaki, H.; Li, C.; Chang, Y.M.; Alnami, I.; Syong, W.R.; et al. Oriented lateral growth of two-dimensional materials on c-plane sapphire. *Nat. Nanotechnol.* **2023**, *18*, 1289–1294. [CrossRef] [PubMed]
28. Panasyuk, G.P.; Azarova, L.A.; Belan, V.N.; Semenov, E.A.; Danchevskaya, M.N.; Voroshilov, I.L.; Kozerozhets, I.V.; Pershikov, S.A. Preparation of fine-grained corundum powders with given properties: Crystal size and habit control. *Theor. Found. Chem. Eng.* **2018**, *52*, 879–886. [CrossRef]
29. Zhu, Z.; Gao, Y.; Shi, Z.; Zhang, X. Study on surface characteristics of as-sawn sapphire crystal wafer considering diamond saw wire wear. *Wear* **2023**, *530–531*, 205037. [CrossRef]
30. Hsieh, C.H.; Chang, C.Y.; Hsiao, Y.K.; Chen, C.C.A.; Tu, C.C.; Kuo, H.C. Recent advances in silicon carbide chemical mechanical polishing technologies. *Micromachines* **2022**, *13*, 1752. [CrossRef]
31. Ng, C.K.; Chen, C.; Yang, Y.; Zhang, F.; Ju, B.F.; Chen, Y.L. Femtosecond laser micro-machining of three-dimensional surface profiles on flat single crystal sapphire. *Opt. Laser Technol.* **2024**, *170*, 110205. [CrossRef]
32. Chen, J.; Lu, X.; Li, Z.; Wen, Q.; Lu, J.; Jiang, F. Anisotropy of material removal during laser-induced plasma assisted ablation of sapphire. *Ceram. Int.* **2022**, *48*, 13880–13889. [CrossRef]
33. Dang, G.T.; Yasuoka, T.; Kawaharamura, T. Sub-μm features patterned with laser interference lithography for the epitaxial lateral overgrowth of α-Ga_2O_3 via mist chemical vapor deposition. *Appl. Phys. Lett.* **2021**, *119*, 041902. [CrossRef]
34. Uhlmann, E.; List, M.; Patraschkov, M.; Tracht, G. A new process design for manufacturing sapphire wafers. *Precis. Eng.* **2018**, *53*, 146–150. [CrossRef]
35. Xu, Y.; Lu, J.; Xu, X.; Chen, C.C.A.; Lin, Y. Study on high efficient sapphire wafer processing by coupling SG-mechanical polishing and GLA-CMP. *Int. J. Mach. Tools Manuf.* **2018**, *130–131*, 12–19. [CrossRef]
36. Zhu, H.; Tessaroto, L.A.; Sabia, R.; Greenhut, V.A.; Smith, M.; Niesz, D.E. Chemical mechanical polishing (CMP) anisotropy in sapphire. *Appl. Surf. Sci.* **2004**, *236*, 120–130. [CrossRef]
37. Wang, J.; Liu, Y.L.; Tan, B.M.; Li, W.W.; Zhou, J.W. Fine polishing of sapphire substrates. *Microelectronics* **2006**, *36*, 46–48.
38. Herzog, A.H.; Walsh, R.J. Process for Polishing Semi-Conductor Materials. U.S. Patent 3170273 A, 23 February 1965.
39. Krishnan, M.; Nalaskowski, J.W.; Cook, L.M. Chemical mechanical planarization: Slurry chemistry, materials and mechanisms. *Chem. Rev.* **2010**, *110*, 178–204. [CrossRef]
40. Sharma, S.; Favela, C.A.; Yu, B.; Galstyan, E.; Selvamanickam, V. Conversion efficiency improvement of ELO GaAs solar cell, deposited on water soluble sacrificial buffer. *Surf. Coat. Technol.* **2023**, *456*, 129282. [CrossRef]
41. Lai, S.M.; Chen, Y.Y.; Liu, C.P.; Hsieh, C.K.; Lin, J.Y. Degradation of inhibitor in alkaline cleaning solution for post-Cu CMP cleaning. *Surf. Coat. Technol.* **2018**, *350*, 1080–1084. [CrossRef]

42. Zhou, Y.; Pan, G.; Shi, X.; Gong, H.; Luo, G.; Gu, Z. Chemical mechanical planarization (CMP) of on-axis Si-face SiC wafer using catalyst nanoparticles in slurry. *Surf. Coat. Technol.* **2014**, *251*, 48–55. [CrossRef]
43. Wei, K.H.; Wang, Y.S.; Liu, C.P.; Chen, K.W.; Wang, Y.L.; Cheng, Y.L. The influence of abrasive particle size in copper chemical mechanical planarization. *Surf. Coat. Technol.* **2013**, *231*, 543–545. [CrossRef]
44. Lin, Z.C.; Chen, C.C. Distribution of polishing times for a wafer with different patterned polishing pads during CMP and CCMP. *Surf. Coat. Technol.* **2010**, *204*, 3101–3107. [CrossRef]
45. Bun-Athuek, N.; Takazaki, H.; Yoshimoto, Y.; Khajornrungruang, P.; Yasunaga, T.; Suzuki, K. Effects of mixed ultrafine colloidal silica particles on chemical mechanical polishing of sapphire. *Jpn. J. Appl. Phys.* **2018**, *57*, 07MD03. [CrossRef]
46. Liu, L.; Zhang, Z.; Wu, B.; Hu, W.; Meng, F.; Li, Y. A review: Green chemical mechanical polishing for metals and brittle wafers. *J. Phys. D Appl. Phys.* **2021**, *54*, 373001. [CrossRef]
47. Zhang, Y.; Lin, B.; Li, Z.C. An overview of recent advances in chemical mechanical polishing (CMP) of sapphire substrates. *ECS Trans.* **2013**, *52*, 495–500. [CrossRef]
48. Cao, L.; Zhang, X.; Yuan, J.; Guo, L.; Hong, T.; Hang, W.; Ma, Y. Study on the influence of sapphire crystal orientation on its chemical mechanical polishing. *Appl. Sci.* **2020**, *10*, 8065. [CrossRef]
49. Zhou, Y.; Pan, G.S.; Shi, X.L.; Gong, H.; Zou, C.L.; Tang, J.N. Atomic step morphology research of LED sapphire substrate polishing surface and its periodicity. *Opt. Precis. Eng.* **2017**, *25*, 100–106. (In Chinese) [CrossRef]
50. Zhou, Y.; Pan, G.; Shi, X.; Gong, H.; Xu, L.; Zou, C. AFM and XPS studies on material removal mechanism of sapphire wafer during chemical mechanical polishing (CMP). *J. Mater. Sci. Mater. Electron.* **2015**, *26*, 9921–9928. [CrossRef]
51. Shi, X.; Pan, G.; Zhou, Y.; Xu, L.; Zou, C.; Gong, H. A study of chemical products formed on sapphire (0001) during chemical-mechanical polishing. *Surf. Coat. Technol.* **2015**, *270*, 206–220. [CrossRef]
52. Shi, X.; Xu, L.; Zhou, Y.; Zou, C.; Wang, R.; Pan, G. An in situ study of chemical-mechanical polishing behaviours on sapphire (0001) via simulating the chemical product-removal process by AFM-tapping mode in both liquid and air environments. *Nanoscale* **2018**, *10*, 19692. [CrossRef] [PubMed]
53. Zhang, Z.; Liu, W.; Song, Z.; Hu, X. Two-step chemical mechanical polishing of sapphire substrate. *J. Electrochem. Soc.* **2010**, *157*, H688–H691. [CrossRef]
54. Vovk, E.A.; Budnikov, A.T.; Dobrotvorskaya, M.V.; Krivonogov, S.I.; Dan'ko, A.Y. Mechanism of the interaction between Al_2O_3 and SiO_2 during the chemical-mechanical polishing of sapphire with silicon dioxide. *J. Surf. Investig. X-ray Synchrotron Neutron Tech.* **2012**, *6*, 115–121. [CrossRef]
55. Yu, H.; Tang, X.; Kong, X.; Li, X.; Li, Y.; Xi, M.; Chang, T.; Meng, D.; Yang, S.; Guo, W.; et al. Electrostatic self-assembled composite abrasives for chemical mechanical polishing of A-plane sapphire. *ECS J. Solid State Sci. Technol.* **2021**, *10*, 114002. [CrossRef]
56. Zhang, Z.; Yan, W.; Zhang, L.; Liu, W.; Song, Z. Effect of mechanical process parameters on friction behavior and material removal during sapphire chemical mechanical polishing. *Microelectron. Eng.* **2011**, *88*, 3020–3023. [CrossRef]
57. Lee, H.; Jeong, H. A wafer-scale material removal rate profile model for copper chemical mechanical planarization. *Int. J. Mach. Tools Manuf.* **2011**, *51*, 395–403. [CrossRef]
58. Oh, S.; Seok, J. An integrated material removal model for silicon dioxide layers in chemical mechanical polishing processes. *Wear* **2009**, *266*, 839–849. [CrossRef]
59. Zhao, G.; Wei, Z.; Wang, W.; Feng, D.; Xu, A.; Liu, W.; Song, Z. Review on modeling and application of chemical mechanical polishing. *Nanotechnol. Rev.* **2020**, *9*, 182–189. [CrossRef]
60. Xu, W.; Cheng, Y.; Zhong, M. Effects of process parameters on chemical-mechanical interactions during sapphire polishing. *Microelectron. Eng.* **2019**, *216*, 111029. [CrossRef]
61. Li, Z.; Deng, Z.; Hu, Y. Effects of polishing parameters on surface quality in sapphire double-sided CMP. *Ceram. Int.* **2020**, *46*, 13356–13364. [CrossRef]
62. Zhang, Z.; Liu, J.; Hu, W.; Zhang, L.; Xie, W.; Liao, L. Chemical mechanical polishing for sapphire wafers using a developed slurry. *J. Manuf. Process.* **2021**, *62*, 762–771. [CrossRef]
63. Yu, Q.; Liu, D.; Chen, T. Chemico-mechanical polishing technique of monocrystal sapphire substrate wafer. *Surf. Technol.* **2017**, *46*, 253–261. (In Chinese)
64. Wang, H.B.; Yu, Q.C.; Liu, W.L.; Song, Z.T.; Zhang, K.L. Process conditions affected chemical mechanical polishing (CMP) on sapphire. *J. Funct. Mater. Devices* **2010**, *16*, 206–210. (In Chinese)
65. Chen, G.; Chen, F.; Ni, Z.; Bai, Y. Study on chemical mechanical polishing of A-plane sapphire wafer. *Electroplat. Finish.* **2023**, *42*, 75–82. (In Chinese)
66. Lin, Z.C.; Huang, W.S.; Tsai, J.S. A study of material removal amount of sapphire wafer in application of chemical mechanical polishing with different polishing pads. *J. Mech. Sci. Technol.* **2012**, *26*, 2353–2364. [CrossRef]
67. Zhu, H.; Niesz, D.E.; Greenhut, V.A. The effect of abrasive hardness on the chemical-assisted polishing of (0001) plane sapphire. *J. Mater. Res.* **2005**, *20*, 504–520. [CrossRef]
68. Wang, H.; Zhang, Z.; Lu, S. Study of several silica properties influence on sapphire CMP. *J. Electr. Eng. Technol.* **2018**, *13*, 886–891.
69. Hu, X.; Song, Z.; Pan, Z.; Liu, W.; Wu, L. Planarization machining of sapphire wafers with boron carbide and colloidal silica as abrasives. *Appl. Surf. Sci.* **2009**, *255*, 8230–8234. [CrossRef]
70. Xiong, W.; Chu, X.; Dong, Y.; Lei, B.; Ye, M.; Sun, W. Effect of different abrasives on sapphire chemical-mechanical polishing. *J. Synth. Cryst.* **2013**, *42*, 1064–1106. (In Chinese)

71. Zhong, M.; Yuan, R.; Li, X.; Chen, J.; Xu, W. Effects of abrasive particles and pads' characteristics on ultrasonic assisted chemical mechanical polishing for sapphire. *China Surf. Eng.* **2018**, *31*, 125–132. (In Chinese)
72. Gao, S.; Kang, R.K.; Jin, Z.J.; Dong, Z.G. Research on the polishing performance of CMP slurry for the sapphire crystal. *Adv. Mater. Res.* **2011**, *325*, 457–463. [CrossRef]
73. Zhang, Z.; Jin, Z.; Guo, J. The effect of the interface reaction mode on chemical mechanical polishing. *CIRP J. Manuf. Sci. Technol.* **2020**, *31*, 539–547. [CrossRef]
74. Kozerozhets, I.; Semenov, E.; Kozlova, L.; Ioni, Y.; Avdeeva, V.; Ivakin, Y. Mechanism to form nanosized oxides when burning aqueous carbohydrate salt solutions. *Mater. Chem. Phys.* **2023**, *309*, 128387. [CrossRef]
75. Dong, Y.; Lei, H.; Liu, W.; Chen, Y. Preparation of ellipsoidal rod-shaped silica nanocomposite abrasives by Chromium ion/PEG200 induced method for sapphire substrates chemical mechanical polishing. *J. Alloys Compd.* **2019**, *777*, 1294–1303. [CrossRef]
76. Seyedi, S.S.; Shabgard, M.R.; Mousavi, S.B.; Heris, S.Z. The impact of SiC, Al_2O_3, and B_2O_3 abrasive particles and temperature on wear characteristics of 18Ni (300) maraging steel in abrasive flow machining (AFM). *Int. J. Hydrog. Energy* **2021**, *46*, 33991–34001. [CrossRef]
77. Zhang, Z.; Zhang, W.; Zhang, S.; Yan, W. Study on chemical mechanical polishing performances of sapphire wafer (0001) using silica-based slurry. *ECS J. Solid State Sci. Technol.* **2017**, *6*, P723–P727. [CrossRef]
78. Liu, J.; Liu, Y.; Xiang, X.; Bian, N. Effects of abrasive on removal rate of sapphire substrate. *Semicond. Technol.* **2010**, *35*, 1053–1064. (In Chinese)
79. Lin, Z.C.; Wang, R.Y. Abrasive removal depth for polishing a sapphire wafer by a cross-patterned polishing pad with different abrasive particle sizes. *Int. J. Adv. Manuf. Technol.* **2014**, *74*, 25–36. [CrossRef]
80. Niu, X.H.; Huang, Y.H.; Zhou, J.W.; Han, L.Y.; Yuan, G.H. Influence of nano abrasive on chemical mechanical ultra-precision machining of sapphire substrate surfaces. *Key Eng. Mater.* **2014**, *609–610*, 130–134. [CrossRef]
81. Bun-Athuek, N.; Yoshimoto, Y.; Sakai, K.; Khajornrungruang, P.; Suzuki, K. Study on effect of the surface variation of colloidal silica abrasive during chemical mechanical polishing of sapphire. *Jpn. J. Appl. Phys.* **2017**, *56*, 07KB01. [CrossRef]
82. Park, C.; Kim, H.; Lee, S.; Jeong, H. The influence of abrasive size on high-pressure chemical mechanical polishing of sapphire wafer. *Int. J. Precis. Eng. Manuf. Green Technol.* **2015**, *2*, 157–162. [CrossRef]
83. Yan, W.X.; Zhang, Z.F.; Guo, X.H.; Liu, W.L.; Song, Z.T. Effect of abrasive concentration on chemical mechanical polishing of sapphire. *Chin. Phys. Lett.* **2015**, *32*, 088301. [CrossRef]
84. Chen, G.; Xu, Y.; Ni, Z.; Bai, Y.; Fan, Q.; Chen, Z. Effects of surfactants on the chemical mechanical polishing performance of a-plane sapphire substrates. *ECS J. Solid State Sci. Technol.* **2023**, *12*, 094003. [CrossRef]
85. Dong, Y.; Lei, H.; Chen, Y.; Liu, W.; Xu, L.; Wang, T.; Dai, S. Preparation of irregular silica nanoparticles by the polymer templating for chemical mechanical polishing of sapphire substrates. *J. Electron. Mater.* **2019**, *48*, 4598–4606. [CrossRef]
86. Dong, Y.; Lei, H.; Liu, W. Preparation of irregular silica nano-abrasives for the chemical mechanical polishing behaviour on sapphire substrates. *Micro Nano Lett.* **2019**, *14*, 1328–1333. [CrossRef]
87. Xu, L.; Lei, H.; Wang, T.; Dong, Y.; Dai, S. Preparation of flower-shaped silica abrasives by double system template method and its effect on polishing performance of sapphire wafers. *Ceram. Int.* **2019**, *45*, 8471–8476. [CrossRef]
88. Dong, Y.; Lei, H.; Liu, W.; Wang, T.; Xu, L. Preparation of non-spherical silica composite abrasives by lanthanum ion-induced effect and its chemical-mechanical polishing properties on sapphire substrates. *J. Mater. Sci.* **2018**, *53*, 10732–10742. [CrossRef]
89. Zhang, B.; Lei, H.; Chen, Y. Preparation of Ag_2O modified silica abrasives and their chemical mechanical polishing performances on sapphire. *Friction* **2017**, *5*, 429–436. [CrossRef]
90. Lei, H.; Liu, T.; Xu, L. Synthesis of Sm-doped colloidal SiO_2 composite abrasives and their chemical mechanical polishing performances on sapphire substrates. *Mater. Chem. Phys.* **2019**, *237*, 121819. [CrossRef]
91. Lei, H.; Tong, K.; Wang, Z. Preparation of Ce-doped colloidal SiO_2 composite abrasives and their chemical mechanical polishing behavior on sapphire substrates. *Mater. Chem. Phys.* **2016**, *172*, 26–31. [CrossRef]
92. Lei, H.; Tong, K.; Zhang, B.; Chen, Y. Preparation of monodisperse Ti-doped colloidal SiO_2 composite abrasives and their chemical mechanical polishing performances on sapphire substrates. *ECS J. Solid State Sci. Technol.* **2016**, *5*, 674–679. [CrossRef]
93. Lei, H.; Tong, K. Preparation of La-doped colloidal SiO_2 composite abrasives and their chemical mechanical polishing behavior on sapphire substrates. *Precis. Eng.* **2016**, *44*, 124–130. [CrossRef]
94. Ma, P.; Lei, H.; Chen, R. Preparation of cobalt-doped colloidal silica abrasives and their chemical mechanical polishing performances on sapphire. *Micro Nano Lett.* **2015**, *10*, 657–661. [CrossRef]
95. Lei, H.; Gu, Q.; Chen, R.; Wang, Z. Preparation of Fe-doped colloidal SiO_2 abrasives and their chemical mechanical polishing behavior on sapphire substrates. *Appl. Opt.* **2015**, *54*, 7188–7194. [CrossRef]
96. Lei, H.; Gu, Q. Preparation of Cu-doped colloidal SiO_2 abrasives and their chemical mechanical polishing behavior on sapphire substrates. *J. Mater. Sci. Mater. Electron.* **2015**, *26*, 10194–10200. [CrossRef]
97. Ma, P.; Lei, H.; Chen, Y.; Chen, R. Preparation of Ni-Doped colloidal silica abrasives and their chemical mechanical polishing performances on sapphire. *ECS J. Solid State Sci. Technol.* **2016**, *5*, 132–136. [CrossRef]
98. Lei, H.; Huang, L.; Gu, Q. Synthesis of Zn-doped colloidal SiO_2 abrasives and their applications in sapphire chemical mechanical polishing slurry. *J. Mater. Sci. Mater. Electron.* **2017**, *28*, 1229–1237. [CrossRef]
99. Zhou, C.; Xu, X.; Dai, L.; Gong, H.; Lin, S. Chemical-mechanical polishing performance of core-shell structured polystyrene@ceria/nanodiamond ternary abrasives on sapphire wafer. *Ceram. Int.* **2021**, *47*, 31691–31701. [CrossRef]

100. Wang, T.; Lei, H.; Dong, Y.; Xu, L.; Dai, S. Highly efficient removal of sapphire by composite nanoabrasive with novel inorganic polyelectrolyte as a binder. *J. Alloys Compd.* **2019**, *782*, 709–715. [CrossRef]
101. Wang, T.; Lei, H. Novel polyelectrolyte-Al_2O_3/SiO_2 composite nanoabrasives for improved chemical mechanical polishing (CMP) of sapphire. *J. Mater. Res.* **2019**, *34*, 1073–1082. [CrossRef]
102. Yin, D.; Niu, X.; Zhang, K.; Wang, J.; Cui, Y. Preparation of MgO doped colloidal SiO_2 abrasive and their chemical mechanical polishing performance on c-, r- and a-plane sapphire substrate. *Ceram. Int.* **2018**, *44*, 14631–14637. [CrossRef]
103. Dai, S.; Lei, H.; Fu, J. Preparation of SiC/SiO_2 hard core–soft shell abrasive and its CMP behavior on sapphire substrate. *J. Electron. Mater.* **2020**, *49*, 1301–1307. [CrossRef]
104. Xu, Y.; Lu, J.; Xu, X. Study on planarization machining of sapphire wafer with soft-hard mixed abrasive through mechanical chemical polishing. *Appl. Surf. Sci.* **2016**, *389*, 713–720. [CrossRef]
105. Wang, X.; Lei, H. Preparation of γ-alumina/silica core–shell abrasives and their chemical mechanical polishing performances on sapphire substrates. *Micro Nano Lett.* **2018**, *13*, 1315–1320. [CrossRef]
106. Zhang, L.; Wang, H.Q.; Suo, S.X.; Yu, S.M. Preparation of CeO_2/ZrO_2 colloidal SiO_2 composite abrasive and its polishing behavior on sapphire. *Bull. Chin. Ceram. Soc.* **2018**, *37*, 3021–3027. (In Chinese)
107. Zhou, C.; Xu, X.Y.; Lin, S.T.; Yao, Y.F. Preparation of DND@CeO_2 core-shell abrasives and their chemical mechanical polishing performances on sapphire wafers. *Min. Metall. Eng.* **2021**, *41*, 115–120. (In Chinese)
108. Bai, L.S.; Xiong, W.; Chu, X.F.; Dong, Y.P.; Zhang, W.B. Preparation of nano SiO_2/CeO_2 composite particles and their applications to CMP on sapphire substrates. *Opt. Precis. Eng.* **2014**, *22*, 1189–1295. (In Chinese)
109. Wang, H.; Yang, J.; Lu, S.; Zhang, Z.; Jiang, X.; Wang, F.; Fan, M.; Peng, Y. Effect of particle hybrid on sapphire polishing performance. *Lubr. Eng.* **2018**, *43*, 43–54. (In Chinese)
110. Park, C.; Kim, H.; Cho, H.; Lee, T.; Kim, D.; Lee, S.; Jeong, H. Efect of relative surface charge of colloidal silica and sapphire on removal rate in chemical mechanical polishing. *Int. J. Precis. Eng. Manuf. Green Technol.* **2019**, *6*, 339–347. [CrossRef]
111. Liu, T.; Lei, H. Nd^{3+}-doped colloidal SiO_2 composite abrasives: Synthesis and the effects on chemical mechanical polishing (CMP) performances of sapphire wafers. *Appl. Surf. Sci.* **2017**, *413*, 16–26. [CrossRef]
112. Wang, W.; Xu, Q.; Liu, W.; Song, Z. Effect of particle size distribution, pH, and Na^+ concentration on the chemical mechanical polishing of sapphire and 4H-SiC (0001). *ECS J. Solid State Sci. Technol.* **2022**, *11*, 044004. [CrossRef]
113. Yin, D.; Niu, X.; Yang, L.; Zhang, K.; Wang, J.; Cui, Y.; Wang, R. Effect of $Sr(OH)_2$ as a pH regulator on different plane sapphire substrate chemical mechanical polishing. *ECS J. Solid State Sci. Technol.* **2019**, *8*, 63–69. [CrossRef]
114. Wang, J.; Niu, X.; Zhao, X.; Liu, Y. Effect of a pH regulator on sapphire substrate CMP. *ECS J. Solid State Sci. Technol.* **2017**, *6*, 832–838. [CrossRef]
115. Deng, H.; Zhong, M.; Xu, W. Investigation of green alkaline pH regulators on sapphire UV-CMP. *Tribol. Int.* **2023**, *178*, 108047. [CrossRef]
116. Yan, W.; Zhang, Z.; Guo, X.; Liu, W.; Song, Z. The effect of pH on sapphire chemical mechanical polishing. *ECS J. Solid State Sci. Technol.* **2015**, *4*, 108–111. [CrossRef]
117. Xie, W.; Zhang, Z.; Liao, L.; Liu, J.; Su, H.; Wang, S.; Guo, D. Green chemical mechanical polishing of sapphire wafers using a novel slurry. *Nanoscale* **2020**, *12*, 22518. [CrossRef]
118. Qu, M.; Niu, X.; Hou, Z.; Yan, H.; Luo, F. Effect of hydroxy carboxylates as complexing agent on improving chemical mechanical polishing performance of M-plane sapphire and action mechanism analysis. *Ceram. Int.* **2023**, *49*, 9622–9631. [CrossRef]
119. Zhang, W.; Lei, H.; Liu, W.; Zhang, Z. Effect of the carboxyl group number of the complexing agent on polishing performance of alumina slurry in sapphire CMP. *Ceram. Int.* **2023**, *49*, 13687–13697. [CrossRef]
120. Qu, M.; Niu, X.; Hou, Z.; Yan, H.; Luo, F.; Zhang, Y.; Zhu, Y. Effect of chitosan oligosaccharide as a complexing agent on chemical mechanical polishing performance of c-, a-, and r-plane sapphire substrate. *ECS J. Solid State Sci. Technol.* **2022**, *11*, 104005. [CrossRef]
121. Zhao, X.; Niu, X.; Wang, J.; Yin, D.; Yao, C. Role of a new type chelating agent in chemical mechanical polishing of r-plane sapphire substrate. *ECS J. Solid State Sci. Technol.* **2017**, *6*, 618–625. [CrossRef]
122. Xiong, W.; Bai, L.; Chu, X.; Dong, Y.; Chen, J.; Bi, L.; Ye, M. Effect of chelating agent on chemical mechanical polishing quality of sapphire. *Mech. Sci. Technol. Aerosp. Eng.* **2014**, *33*, 1027–1030. (In Chinese)
123. Niu, X.; Liu, X.; Wang, S.; Tan, B. High precision finishing technique of sapphire substrate surface for photoconducting device. *Mater. Sci. Forum* **2011**, *663–665*, 80–83. [CrossRef]
124. Bai, Y.W.; Chen, G.M.; Teng, K.; Ni, Z.F. Effect of cationic surfactant on chemical mechanical polishing efficiency of a-plane sapphire. *J. Synth. Cryst.* **2018**, *47*, 470–475. (In Chinese)
125. Chen, G.; Du, C.; Ni, Z.; Bai, Y.; Liu, Y.; Zhao, Y. Effect of amphoteric surfactant on the chemical mechanical polishing of A-plane sapphire wafer. *Modern Manuf. Eng.* **2020**, *483*, 83–87. (In Chinese)
126. Zhao, X.; Niu, X.; Yin, D.; Wang, J.; Zhang, K. Research on r-plane sapphire substrate CMP removal rate based on a new-type alkaline slurry. *ECS J. Solid State Sci. Technol.* **2018**, *7*, P135–P141. [CrossRef]
127. Deng, H.; Zhong, M.; Xu, W. Effects and mechanisms of different types of surfactants on sapphire ultrasonic polishing. *Tribol. Int.* **2023**, *187*, 108734. [CrossRef]
128. Zhang, Z.; Liu, W.; Song, Z. Particle size and surfactant effects on chemical mechanical polishing of glass using silica-based slurry. *Appl. Opt.* **2010**, *49*, 5480–5485. [CrossRef]

129. Cui, Y.; Niu, X.; Zhou, J.; Wang, Z.; Wang, R.; Zhang, J. Effect of chloride ions on the chemical mechanical planarization efficiency of sapphire substrate. *ECS J. Solid State Sci. Technol.* **2019**, *8*, 488–495. [CrossRef]
130. Lu, Y.; Niu, X.; Yang, C.; Huo, Z.; Cui, Y.; Zhou, J.; Wang, Z. Effect of potassium persulfate as an additive on chemical mechanical polishing performance on c-, a- and r-plane sapphire. *ECS J. Solid State Sci. Technol.* **2020**, *9*, 064006. [CrossRef]
131. Xu, L.; Zou, C.; Shi, X.; Pan, G.; Luo, G.; Zhou, Y. Fe-N_x/C assisted chemical-mechanical polishing for improving the removal rate of sapphire. *Appl. Surf. Sci.* **2015**, *343*, 115–120. [CrossRef]
132. Xu, L.; Zhang, X.; Kang, C.; Wang, R.; Zou, C.; Zhou, Y.; Pan, G. Preparation of a novel catalyst ($SoFe^{III}$) and its catalytic performance towards the removal rate of sapphire substrate during CMP process. *Tribol. Int.* **2018**, *120*, 99–104. [CrossRef]
133. Xu, W.; Lu, X.; Pan, G.; Lei, Y.; Luo, J. Effects of the ultrasonic flexural vibration on the interaction between the abrasive particles; pad and sapphire substrate during chemical mechanical polishing (CMP). *Appl. Surf. Sci.* **2011**, *257*, 2905–2911. [CrossRef]
134. Xu, W.; Lu, X.; Pan, G.; Lei, Y.; Luo, J. Ultrasonic flexural vibration assisted chemical mechanical polishing for sapphire substrate. *Appl. Surf. Sci.* **2010**, *256*, 3936–3940. [CrossRef]
135. Zhou, M.; Cheng, Y.; Zhong, M.; Xu, W. Macro and micro-nano machining mechanism for ultrasonic vibration assisted chemical mechanical polishing of sapphire. *Appl. Surf. Sci.* **2023**, *640*, 158343. [CrossRef]
136. Deng, H.; Zhong, M.; Xu, W. Effects of different dispersants on chemical reaction and material removal in ultrasonic assisted chemical mechanical polishing of sapphire. *ECS J. Solid State Sci. Technol.* **2022**, *11*, 033007. [CrossRef]
137. Zhou, M.; Zhong, M.; Xu, W. Novel model of material removal rate on ultrasonic-assisted chemical mechanical polishing for sapphire. *Friction* **2023**, *11*, 2073–2090. [CrossRef]
138. Li, Z.; Deng, Z.; Ge, J.; Zhuo, R.; Wan, L. Material removal rate prediction for sapphire double-sided CMP based on RSM-SVM. *ECS J. Solid State Sci. Technol.* **2022**, *11*, 084002. [CrossRef]
139. Li, Z.; Deng, Z.; Ge, J.; Liu, T.; Wan, L. Experimental and theoretical analysis of single-sided and double-sided chemical mechanical polishing of sapphire wafers. *Int. J. Adv. Manuf. Technol.* **2022**, *119*, 5095–5106. [CrossRef]

Disclaimer/Publisher's Note: The statements, opinions and data contained in all publications are solely those of the individual author(s) and contributor(s) and not of MDPI and/or the editor(s). MDPI and/or the editor(s) disclaim responsibility for any injury to people or property resulting from any ideas, methods, instructions or products referred to in the content.